AD-755 099

ESTIMATING WATER-SHOCK-INDUCED AIRBLAST FROM DETONATIONS IN A MEDIUM OVERLAIN WITH WATER

Charles M. Snell

Army Engineer Waterways Experiment Station
Livermore, California

April 1972

TECHNICAL REPORT E-72-16

ESTIMATING WATER-SHOCK-INDUCED AIRBLAST FROM DETONATIONS IN A MEDIUM OVERLAIN WITH WATER

by

Charles M. Snell

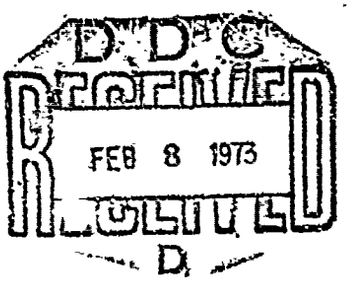

April 1972

U. S. Army Engineer Waterways Experiment Station
Explosive Excavation Research Laboratory
Livermore, California

Approved for public release; distribution unlimited.

65
R

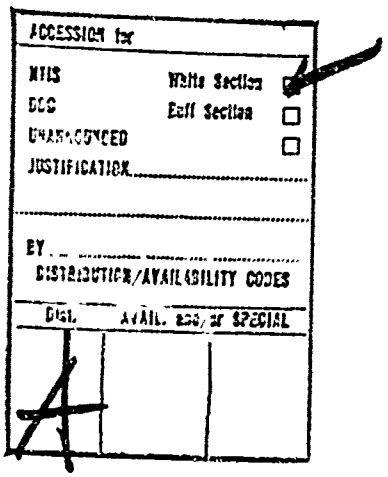

Destroy this report when no longer needed.
Do not return it to the originator.

The findings in this report are not to be construed as an official Department of the Army position unless so designated by other authorized documents.

Printed in USA. Available from Defense Documentation Center,
Cameron Station, Alexandria, Virginia 22314 or
National Technical Information Service,
US Department of Commerce,
Springfield, Virginia 22151

UNCLASSIFIED

Security Classification

DOCUMENT CONTROL DATA - R & D

(Security classification of title, body of abstract and indexing annotation must be entered when the overall report is classified)

1. ORIGINATING ACTIVITY (Corporate author) U. S. Army Engineer Waterways Experiment Station Explosive Excavation Research Laboratory	2a. REPORT SECURITY CLASSIFICATION UNCLASSIFIED 2b. GROUP

3. REPORT TITLE

Estimating Water-Shock-Induced Airblast from Detonations in a Medium Overlain with Water

4. DESCRIPTIVE NOTES (Type of report and inclusive dates)

Final Report, April 1972

5. AUTHOR(S) (First name, middle initial, last name)

Charles M. Snell

6. REPORT DATE	7a. TOTAL NO. OF PAGES	7b. NO. OF REFS
April 1972	65	18

8a. CONTRACT OR GRANT NO.	9a. ORIGINATOR'S REPORT NUMBER(S)
N/A b. PROJECT NO.	TR E-72-16
c.	9b. OTHER REPORT NO(S) (Any other numbers that may be assigned this report)
d.	

10. DISTRIBUTION STATEMENT

Distribution unlimited

11. SUPPLEMENTARY NOTES	12. SPONSORING MILITARY ACTIVITY

13. ABSTRACT

A geometrical shock wave transmission model is used to determine water surface peak spall velocities above single-charge cratering detonations in a medium overlain by a thin-to-moderately-thick layer of water. These velocities, in conjunction with an acoustic simple source treatment, predict the water-shock-induced airblast from such events. Required input data include the acoustic impedance and shock wave transmission properties of the cratering medium in the inelastic and elastic regions. The method is intended to predict far-field airblast in the "low" overpressure regime, for which case the acoustic simple source treatment is valid. This regime is of direct interest in determining airblast damage from typical explosive cratering events. The method is expected to be less accurate for extremely high overpressure levels and supersonic peak spall velocities, which require non-acoustic analysis.

A computer code called "MULTIMEDIA" is included with this report as an aid to numerical prediction calculations. Predictions made using the code are compared with the limited airblast data available for underwater cratering tests. Results indicate that the basic assumptions of the method are correct. Further improvements in the prediction scheme and input parameters will be possible as more data become available.

DD FORM 1 NOV 68 1473

UNCLASSIFIED

Security Classification

14. KEY WORDS	LINK A		LINK B		LINK C	
	ROLE	WT	ROLE	WT	ROLE	WT
Airblast Overpressures						
Airblast Prediction						
Underground Explosions						
Underwater Explosions						
Explosive Excavation						
Explosive Engineering						
Theoretical Airblast Prediction						
Ground-Shock-Induced Airblast Prediction						
Water-Shock-Induced Airblast Prediction						
Spall Velocities						
Spall Mechanisms						
Peak Vertical Spall Velocity Prediction						

TID-4500, UC-35

TECHNICAL REPORT E-72-16

ESTIMATING WATER-SHOCK-INDUCED AIRBLAST FROM DETONATIONS IN A MEDIUM OVERLAIN WITH WATER

CHARLES M. SNELL

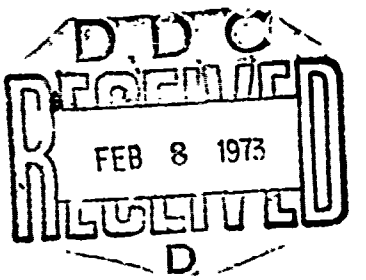

U.S. ARMY ENGINEER WATERWAYS EXPERIMENT STATION
EXPLOSIVE EXCAVATION RESEARCH LABORATORY
Livermore, California

MS. date: April 1972

Preface

The U.S. Army Engineer Waterways Experiment Station (USAEWES) Explosive Excavation Research Laboratory (EERL) was the USAEWES Explosive Excavation Research Office (EERO) prior to 21 April 1972. Prior to 1 August 1971 the organization was known as the USAE Nuclear Cratering Group.

EERL is conducting a program of research in topical areas critical to the overall technology titled "explosive excavation." The prediction of airblast overpressures is one of these topical areas. This report presents a shock wave transmission model that is used to determine peak water surface spall velocities above single-charge cratering detonations in a medium overlain by a layer of water. These spall velocities are then used to predict far-field peak airblast overpressures. The work was performed in conjunction with studies of airblast safety by the EERL Environmental Effects Division. It was funded by the Office of the Chief of Engineers (OCE) appropriation 96x3121, General Investigations.

The Directors of EERL during the preparation of this report were LTC R. L. LaFrenz and LTC R. R. Mills.

The author wishes to thank Mr. E. J. Leahy, Chief, Environmental Effects Division, for his assistance and suggestions throughout the airblast investigation program. Appreciation is also expressed to MAJ R. H. Gates for providing data and useful discussions concerning media characteristics. Mr. B. B. Redpath, Mr. W. C. Day, and CPT D. E. Burton provided additional data concerning properties of saturated media. Dr. A. Sakurai of the U.S. Army Engineer Waterways Experiment Station Weapons Effects Laboratory also presented a number of helpful comments and suggested possible areas for future research.

Contents

TABLES (continued)

Nomenclature

C_a = Undisturbed sonic velocity in air at sea level (ft/sec).

C_r = Compressional elastic wave velocity in the cratering medium (ft/sec).

C_w = Undisturbed sonic velocity in water (ft/sec).

D_{ap} = Total apparent charge depth, allowing for refraction at the rock-water interface.

D_r = Depth of burial of the charge in the cratering medium (ft).

D_w = Depth of the water layer above the cratering medium (ft).

dob = Scaled depth of burial of a charge in a one-layer cratering medium (no overlying water layer) = Depth of burial/$W^{1/3}$, (expressed in ft/$kt^{1/3}$).

h = Vertical height above the water surface of an elevated far-field point at which ΔP predictions are desired.

M = Mach number of the air shock at SGZ.

$P_{ambient}$ = Ambient air pressure at SGZ, just above the water surface.

P_{STP} = Ambient air pressure at standard sea level conditions = 1013 mbar = 14.68 psi.

ΔP_{local} = Peak local airblast overpressure (excess above ambient air pressure) at the rising water surface in the near field ($R_w/(D_r + D_w) < 1$ to 2).

ΔP_{rock} = Peak radial stress in the rock layer (excess above ambient pressure); ΔP_{rock} is a function of scaled range from the shot point.

$\Delta P(R_w)$ = Peak airblast overpressure (excess above ambient air pressure) at the water surface level in the <u>far field</u> ($R_w/(D_r + D_w) \gtrsim 2$).

ΔP_{water} = Peak shock pressure (excess above ambient hydrostatic pressure) in the water layer; calculated for locations just below the water surface.

ΔP_0 = Peak <u>local</u> or near-field airblast overpressure (excess above ambient air pressure) <u>at SGZ</u>.

p = Exponent describing the dependence of rock surface vertical spall velocity on inverse dimensionless slant range (D_r/S_r) from shot point. The quantity "p" applies to free rock surface velocities (no overlying water layer).

R_s = Scaled range from shot point in the rock layer (ft/$kt^{1/3}$).

R_w = Water surface range: distance from SGZ, measured along the water-air interface (ft).

SGZ = Surface ground zero; the point at the water-air interface (or rock-air interface) vertically above the shot point.

S_r = Slant range from shot point to a location on the rock-water interface (ft).

S_w = Slant range from a point on the rock-water interface to a point on the water-air interface along a path of shock propagation (ft).

T = Pressure transmission factor at the rock-water interface; ratio of the pressure on the water side of the interface to the pressure on the rock side of the interface at a given location.

U_r = Velocity of propagation of the peak of the radial stress wave in the inelastic region of the cratering medium (ft/sec; U_r is less than the compressional elastic wave velocity for most compressible media of interest for excavation applications.

U_{radial} = Peak radial free-field particle velocity in the cratering medium near an explosion; U_{radial} is a function of scaled range from the shot point.

U_w = Local shock front propagation velocity in water (ft/sec); $U_w \approx C_w$ for peak pressures less than 20,000 psi; $U_w > C_w$ for very high pressures.

V(rock) = Peak vertical spall velocity of a free surface with no overlying water layer. This velocity is not necessarily at SGZ (interface vertically above the shot point) but may be located at any distance from SGZ.

V_{spall} at SGZ $= V_0$(rock) = Peak vertical spall velocity at SGZ for a free surface (that is, for a one-layer medium with no overlying water layer).

V(water) = Peak vertical spall velocity of the water surface layer (as a function of R_w).

V_0(water) = Peak vertical spall velocity of the water surface at or close to SGZ.

W = Yield of a detonation (kt or tons).

α = Uniquely determined constant (for a given detonation) which relates peak airblast overpressure to the dimensionless range in Montan's airblast prediction method.

γ = Ratio of specific heats = 1.4 for an ideal gas.

$\theta_{elevation}$ = Measured elevation angle to an elevated location; angle between the vertical direction and a vector from SGZ to the elevated location.

θ_r = Angle between the direction of shock propagation and the rock-water interface on the rock side of the interface (degrees).

θ_w = Angle between the direction of shock propagation and the rock-water interface on the water side of the interface (degrees).

$\rho_a C_a$ = Acoustic impedance of air under sea level conditions =0.01841 (psi-sec/ft).

$\rho_r C_r$ = Acoustic impedance of the cratering medium in the elastic propagation regime (psi-sec/ft).

$\rho_r U_r$ Impedance of the cratering medium in the inelastic regime, for peak radial stress wave propagation velocity U_r (psi-sec/ft).

$\rho_w C_w$ = Acoustic impedance of water (psi-sec/ft).

Subscripts

a = Air; parameter or quantity for the air layer.

ap = apparent charge (depth), allowing for refraction.

r = rock or cratering medium; parameter or quantity for the rock layer.

R_s = scaled range from shot point in the rock layer ($ft/kt^{1/3}$); equivalent to true range S_r for an assumed yield of 1 kt.

w = water; parameter or quantity for the water layer.

Conversion Factors

British units of measurement used in this report can be converted to metric units as follows:

Multiply	By	To obtain
inches	2.54	centimeters
feet	0.3048	meters
cubic feet	0.02832	cubic meters
cubic yards	0.764555	cubic meters
pounds	0.4535924	kilograms
pounds per square inch	0.00689476	meganewtons per square meter
pounds per cubic foot	16.02	kilograms per cubic meter
Fahrenheit degrees	5/9	Celsius or Kelvin degrees[a]
foot-pounds	0.138255	meter-kilograms

[a]To obtain Celsius (C) temperature readings from Fahrenheit (F) readings, use the following formula: C = (5/9) (F - 32). To obtain Kelvin (K) readings, use: K = (5/9) (F - 32) + 273.15.

ESTIMATING WATER-SHOCK-INDUCED AIRBLAST FROM DETONATIONS IN A MEDIUM OVERLAIN WITH WATER

Section 1. Principles

The method developed in this report predicts water-shock-induced airblast from detonations in cratering media overlain by shallow layers of water. The method utilizes a simplified model of shock transmission through the cratering and water layers in which all pressure pulses are assumed to propagate according to the laws of regular transmission and reflection. The pressure pulses propagating through the water reach the water-air interface and launch a surface spall layer according to the free-surface law (all incident pulses are perfectly reflected as tension waves, doubling the spall launch velocity). The spalled surface induces an airblast pulse in the overlying air. Far-field overpressures near the water surface level are predicted by using the calculated vertical spall velocities. Basic assumptions implicit in the method are discussed below.

Section 2. Assumptions

A spherically divergent detonation shock wave propagates through a two-layered homogeneous quiescent medium (the bottom layer is referred to as "rock" for purposes of convenience; the second layer is water). Transmission and reflection of shock waves at the rock-water and water-air interfaces are described by the acoustic laws for ideal discontinuous waves of infinitesimal amplitude.[1,2] The acoustic laws of regular transmission and reflection generally hold for most cases of interest. In water, for example, shock waves closely follow acoustic behavior at peak pressures up to 10,000 psi when the wave's direction of propagation intersects an interface at angles greater than 60° (Ref. 1). The peak radial stress functions within the cratering medium are assumed to be known. These peak stresses are in turn used to calculate the peak pressures transmitted across the rock-water interface into the water layer. Elastic precursors in the rock layer are ignored. The peak stress wave is indeed a very strongly dominant effect at ranges close to explosions in almost all cratering media of interest.* Next, peak pressures transmitted through the water layer to the water-air

*If precursor pulses should prove dominant in launching the water surface spall for any case, the treatment given below could still be used. However, it would be necessary (1) to determine the peak excess pressure function of the precursor, (2) to substitute that function for the usual peak radial stress function in the rock layer, ΔP_{rock} (at S_r), and (3) to substitute the elastic precursor velocity in rock, C_r, for the inelastic velocity in the rock, U_r (see Section 4).

interface are calculated using semiacoustic transmission equations, which include allowance for spherical aberration and astigmatism of the refracted rays (see Section 5 and Appendix A). It is assumed that the water-air interface acts as a free surface; the water pressure pulses are perfectly reflected as tension waves, and the top portion of the water layer immediately spalls upward as a free surface.[3] The water surface spall mound, in turn, acts as a simple acoustic source of far-field airblast overpressures transmitted into the air layer.[4,5] The entire "direct ray" approach to calculating water pressures and surface spall velocities is based on the assumption that the water layer is sufficiently thin and the cavitational spall launch after peak pressure pulse arrival is sufficiently rapid that direct geometric pulse transmission is a satisfactory approximation. This assumption is equivalent to adopting a local pressure approximation throughout the second layer. The local pressure approximation will be valid only as long as the water layer pressure pulses originating from a broad area of the rock-water interface are not combined into a single or far-field pressure pulse. Combination will not occur if consideration is restricted to water layers not appreciably thicker than the charge burial depth in the underlying rock layer and to the central part of the induced spall velocity field (surface ranges $\lesssim$ a few times the charge burial depth).

Section 3. Accuracy and Range of Applicability

The assumption that transmitted peak stress acts as a discontinuous pressure pulse in launching the spall is not strictly correct. However, it is a useful approximation for obtaining a straightforward mathematical development capable of predicting airblast. The deviations of shock behavior and waveforms in rock from this simple model are such that the method will overestimate peak pressures transmitted into the water that are effective in launching the spall. Thus, the induced surface velocities and airblast will be overpredicted. Likewise, the simple source assumption discussed above may not hold perfectly for the very broad velocity fields induced by charges in water and saturated media. However, breadth of the shockfront tends to cause incomplete reinforcement of local airblast pulses from various parts of the spalled surface. Again, the resulting airblast will be less than the predicted level. This discussion indicates that, given proper input parameters, the method will safely predict the water-shock-induced airblast.

The approach used in this report considers only the transmitted peak stress pulse and the induced peak water surface spall velocities. Therefore, it predicts the water-shock-induced peak airblast. Events at much later times, including the mound disintegration and "blowout" (cavity gas vent), are not considered. Current evidence indicates that the gas vent is very rapidly suppressed with increasing depth of burial for all chemical explosive events in water and in media of 90% or greater saturation. The water-shock-induced (or "ground-shock-induced") airblast component is strongly

dominant for events buried more deeply than 170 ft/kt$^{1/3}$ in water or a saturated medium.[5] It is expected that this component will remain dominant for detonations in most cratering media overlain by water at total depths near or below 170 ft/kt$^{1/3}$. Note that the theory applied here is not appropriate for very shallow detonations, particularly for those shallower than about 80 ft/kt$^{1/3}$. These events give rise to an intense supersonic water plume that penetrates the spall dome at early time and to other venting effects that invalidate a simple spall analysis. Shallow events are discussed more extensively elsewhere,* but consideration here will be restricted to subsonic water interface velocities.

Section 4. Input Data

Application of a two-layer shock wave transmission model requires knowledge of the peak pressures in both layers.[6,8] The acoustic characteristics of each medium[6,7] are also needed in order to determine shock wave transmission behavior at the interface. Necessary parameters include the acoustic impedances (ρC),† which are known for virtually all media. The fundamental parameters are listed in Tables 1 through 4. Tables 1 and 2 give the acoustic impedance, $\rho_w C_w$, and the undisturbed sonic velocity, C_w, in water (as functions of temperature and salinity). Table 3 summarizes a useful scheme for classifying excavation media. Table 4 lists the acoustic impedances and shock wave transmission properties (see below) of several excavation media that may be encountered in underwater applications. For purposes of this report, the term "rock" and the subscripts "rock" and "r" will be used for all cratering media with acoustic impedances greater than that of water.

Table 1. Acoustic impedance of water at atmospheric pressure for several temperatures and salinities.[7]

Salinity, parts per thousand (ppt)[a]	Temperature (°C)			
	0	10	20	30
	Acoustic impedance, $\rho_w C_w$ (psi-sec/ft)			
0	61.98	63.97	65.43	66.49
10	63.08	64.98	66.40	67.42
20	64.19	66.04	67.42	68.39
30	65.29	67.11	68.43	69.36
35	65.87	67.68	68.96	69.85

[a]Seawater salinity = 35 ppt.

*References 12 through 16.

†All impedances in this report are expressed in units of psi-sec/ft, following standard acoustic usage.

Table 2. Sound velocity of water at atmospheric pressure for several temperatures and salinities.[7]

Salinity, parts per thousand (ppt)[a]	Temperature (°C)			
	0	10	20	30
	Sound velocity, C_w (ft/sec)			
0	4601.1	4748.8	4865.8	4956.5
10	4643.7	4787.7	4901.0	4987.9
20	4687.3	4827.6	4937.3	5020.6
30	4732.1	4868.7	4974.7	5054.3
35	4754.9	4889.7	4993.8	5071.5

[a]Seawater salinity = 35 ppt.

Table 3. Media classification for explosive excavation.[10]

I. Media
   A. Common Excavation
      1. Soil
      2. Clay shale
   B. Rock Excavation (requires drilling and blasting to excavate)
      1. Weak rock (less than 4000-psi unconfined compressive strength)
      2. Intermediate-strength rock (4000 to 16,000-psi unconfined compressive strength)
      3. High-strength rock (greater than 16,000-psi unconfined compressive strength)

II. Lithology (rock excavation) or Soil Classification (common excavation) and and Geologic Structure

III. Degree of Saturation or Water Content
   A. Dry (less than 50% saturated or less than 10% water content—common—or less than 3% water content—rock)
   B. Wet (between 50 and 90% saturated or greater than 10% water content—common—or greater than 3% water content—rock)
   C. Saturated (greater than 90% saturated)

Given the fundamental shock wave parameters, one may easily determine peak pressures in water.[7,9] Unfortunately, peak radial stresses in cratering media are more difficult to obtain. The peak stress, ΔP_{rock}, at the rock-water interface is needed in order to calculate the pressure transmitted into the water. Let S_r be the true slant range from shot point to any given location on the rock-water interface. Then ΔP_{rock} will be expressed as a function of S_r. The following are five methods of estimating ΔP_{rock} (at S_r).

Table 4. Properties of several media in which underground explosive tests have been conducted.[5,6]

Medium[a]	ρ_r (g/cm^3)	C_r (ft/sec)	$\rho_r C_r$ in elastic region (psi-sec/ft)	U_r (ft/sec)	$\rho_r U_r$ in inelastic region (psi-sec/ft)	n_r Eq. (1) Inelastic	n_r Eq. (1) Elastic	p (inelastic)[b] Eq. (5b)
Unsaturated high impedance soil with few unfilled voids (alluvium; common)	2.0	7,200	195	4,850	131	3.8	1.3	3
Saturated soil (alluvium; common)	2.35	12,500[c]	397	9,100	289	—	—	<3
Saturated clay shale (bearpaw shale) (weak rock)	2.2	6,400	191	—	—	—	—	2.5
Unsaturated intermediate strength rock (zeolitized tuff)	1.95	7,900	208	6,000	158	—	—	—
Saturated intermediate strength rock (saturated zeolitized tuff)	2.0	9,000	243	8,000	216	—	—	<3
Saturated high strength rock (saturated andesite)	2.35	12,500	395	9,500	300	1.8	1.0[c]	<3[d]
Saturated very weak coral	1.6-1.8	6,300	136-153	<6,300	<136	1.7	1.3[e]	<3[d]
Unsaturated high strength rock (granite)	2 65	18,000	644	13,700	490	2.4	1.1	—
Unsaturated basalt (high strength)	2.6	10,000	351	—	—	—	—	6
Unsaturated rhyolite (intermediate strength)	2.35	up to 8,000	254	—	—	—	—	3+

[a]Some of the media are not saturated; data for these cases will not apply directly to most underwater cratering experiments.

[b]See Ref. 5.

[c]Estimate.

[d]Probable value.

[e]Rough estimate.

a. THEORETICAL CODE CALCULATIONS OF CRATERING DYNAMICS

Theoretical code calculations of cratering dynamics,[8] based on the known characteristics of the cratering medium, can provide values of the peak radial stress.

b. DIRECT MEASUREMENTS OF PEAK RADIAL STRESS

Direct measurements of the peak radial stress for experiments in the given cratering medium would be most useful. Unfortunately, due to the enormous difficulty of performing such measurements very close to an explosion, the available data are incomplete for saturated media.

c. MEASURED FREE-FIELD PEAK RADIAL PARTICLE VELOCITIES

Measured free-field peak radial particle velocities in the given medium can be used to calculate peak radial stresses. Free-field particle velocities have been measured for a wide variety of different media.[6,11] Peak radial particle velocities, U_{radial}, are well-fitted by a relation of the form:

$$U_{radial} = K_1 \left(\text{true range}/W^{1/3}\right)^{-n_r}, \qquad (1)$$

where K_1 and n_r are constants for a given medium, type of explosive, and propagation region. K_1 and n_r have two different values for a given medium-explosive combination; n_r is relatively large in the inelastic or cratering region close to the detonation. This is the region in which permanent displacement, crushing, or cracking of the material takes place. At longer ranges, the stress decreases to a level at which the material responds elastically. Energy is not irreversibly deposited in the medium (although some energy degradation continues to occur due to natural dissipative processes). These longer ranges are referred to as the elastic region of shock propagation; n_r is usually much smaller in the elastic region. The transition between inelastic and elastic propagation occurs at (true range/$W^{1/3}$) ≈ 140 to 700 ft/$kt^{1/3}$ for typical cratering media.[6,11] Experimental data show that $4.0 > n_r > 1.0$ in the inelastic region, and $1.3 > n_r > 1.0$ in the elastic region (Table 4). Given the peak radial particle velocity at a specified range, the peak radial stress, ΔP_{rock}, at that range is:

$$\Delta P_{rock} = U_{radial}\,(\rho_r U_r) \text{ in the inelastic region,} \qquad (2)$$

$$\Delta P_{rock} = U_{radial}\,(\rho_r C_r) \text{ in the elastic region,} \qquad (3)$$

where $\rho_r U_r$ = impedance of the cratering medium in the inelastic regime, for peak radial stress wave velocity U_r; $\rho_r C_r$ = acoustic impedance of the cratering medium in the elastic propagation regime (sonic velocity, C_r). These quantities are approximately constant for a given medium. The ΔP_{rock} calculated above is the increase in stress

above the local ambient pressure (ambient pressure is usually negligible compared to ΔP_{rock}).

Graphs of U_{radial} and ΔP_{rock} as functions of (true range/$W^{1/3}$) are given in Ref. 6 for nuclear explosions in several media. These experimentally derived graphs encompass both the inelastic and elastic regions. A complete discussion of the results is beyond the scope of this report, but values of U_{radial} or ΔP_{rock} for many media may be obtained from the literature.

d. MEASURED PEAK VERTICAL SPALL VELOCITIES

One means of approximating ΔP_{rock} uses measured peak vertical spall velocities at surface ground zero (SGZ) for cratering events with no overlying water layer. (Peak vertical spall velocities should not be confused with late-time gas-acceleration-induced velocities.) Observed peak vertical spall velocities for experiments in a given medium with a given type of explosive are a function of scaled depth of burial (dob = scaled depth of burial; for the one-layer case, with no overlying water layer, dob = rock depth/$W^{1/3}$ = $D_r/W^{1/3}$). The measured peak vertical spall velocities of the rock at SGZ fit a relation of the form:

$$V_{spall\ at\ SGZ} = V_0\ (rock) = K_2\ (dob)^{-m_r}, \tag{4}$$

where K_2 and m_r are constants for a given medium and type of explosive.* $V_{spall\ at\ SGZ}$ relations for various media and explosives are discussed in Ref. 5.

Once the peak vertical spall velocity at a specified scaled depth of burial is known, it may be used to calculate the peak radial particle velocity U_{radial} in the given medium at a scaled range equal to the scaled depth of burial:

$$U_{radial}\ (\text{at true range}/W^{1/3}) = 1/2\ \left[V_{spall\ at\ SGZ}\ (\text{at the given dob})\right]$$
$$= 1/2\ \left[V_0\ (rock)(\text{at the given dob})\right],$$

where (true range/$W^{1/3}$) = dob = $D_r/W^{1/3}$. The U_{radial} thus obtained is substituted into Eq. (2), giving ΔP_{rock}:

$$\Delta P_{rock}\ (\text{at scaled range} = dob) = 1/2\ \left[(\rho_r U_r)\ V_0\ (rock)\right]. \tag{5a}$$

This method currently applies to experiments at cratering depths (but not to deep contained detonations). It gives U_{radial} and ΔP_{rock} in the inelastic region (close ranges, scaled range $\lesssim$ 300 ft/$kt^{1/3}$), and cannot be used for longer ranges. The SGZ peak

*These values are constants for the inelastic region: i.e., for experiments at cratering depths. The values of K_2 and m_r are expected to change for the elastic region (deep contained events).

vertical spall velocities for contained experiments are not always reliable for determining peak radial particle velocities in or near the elastic region. Photographically measured velocities for deep experiments tend to be lower and attenuate faster than true peak particle velocities should, because the surface material does not break apart and spall freely, but responds in a partially elastic fashion. If reliable peak surface velocities for deep contained experiments become available, they may be used in Eqs. (5a) and (3) to obtain ΔP_{rock} at various ranges (substitute $\rho_r C_r$ for $\rho_r U_r$).

e. MEASURED PEAK VERTICAL SPALL VELOCITY PROFILES

One additional method for finding peak pressures in the rock layer is available. This method is related to the procedure described in the previous paragraph, because it utilizes peak vertical spall velocity data for free rock surfaces with no overlying water layer; it differs because it makes use of measured velocities at locations other than SGZ.

Again, let V_0 (rock) be the SGZ peak vertical spall velocity of a free rock surface above a detonation at dob = $D_r/W^{1/3}$. Then, as was shown in Method (d) above, ΔP_{rock} at a scaled range $S_r/W^{1/3}$ equal to the dob is given by:

$$\Delta P_{rock}\left[\text{at } S_r/W^{1/3} = \text{dob}\right] = 1/2\left[(\rho_r U_r)\, V_0\ (\text{rock})\right]. \qquad (5a)$$

Measured V_0 (rock) values may be substituted into this equation to obtain ΔP_{rock} at various ranges. However, the SGZ velocities may not be accurately known over a wide range of dob's. In some cases, the SGZ velocity at one scaled depth of burial and the manner in which the velocity profile decreases moving away from SGZ are known. This information can also be used to derive ΔP_{rock} values, although with somewhat lower accuracy. First, let V(rock) be the peak vertical spall velocity of a free rock surface (no overlying water) at any location other than SGZ. Reference 5 demonstrates that V(rock) is usually well-fitted by an empirical relation of the form:

$$V(\text{rock}) = V_0\ (\text{rock})\left[\frac{D_r}{S_r}\right]^p,$$

where "p" is a medium-dependent exponent that does not vary greatly for detonations at different scaled depths of burial in the same medium. This equation describes the velocity profile of the spall mound launched by the detonation.

Next, let ΔP_{rock} be the peak excess pressure of a shock wave whose direction of propagation intersects a free rock surface at angle θ_r. The spall velocity of the free surface at that location will then be:

$$V(\text{rock}) = \frac{2\Delta P_{rock}}{(\rho_r U_r)} \sin\theta_r,$$

or, substituting from the empirical V(rock) equation,

$$\Delta P_{rock} = 1/2 \left[(\rho_r U_r)\, V(\text{rock}) \frac{1}{\sin \theta_r} \right]$$

$$= 1/2 \left\{ (\rho_r U_r)\, V_0\, (\text{rock}) \left[\frac{D_r}{S_r} \right]^p \frac{1}{\sin \theta_r} \right\};$$

and, since $\sin \theta_r = \left(\frac{D_r}{S_r} \right)$,

$$\Delta P_{rock} \left(\text{at } \frac{S_r}{W^{1/3}} \right) = 1/2 \left\{ (\rho_r U_r)\, V_0\, (\text{rock}) \left[\frac{D_r}{S_r} \right]^{p-1} \right\}. \qquad (5b)$$

Given the SGZ peak vertical spall velocity V_0 (rock) at one scaled depth of burial (dob = $D_r/W^{1/3}$) and the exponent p, Eq. (5b) is used to calculate ΔP_{rock} at any scaled range ($S_r/W^{1/3}$) greater than the dob. This equation is valid within the range of inelastic propagation for a given medium. If one knows the scaled range at which elastic propagation takes over, the peak pressures obtained from Eq. (5b) may be very approximately extrapolated into the elastic region* as $(S_r/W^{1/3})^{-1}$ or $(S_r/W^{1/3})^{-1.2}$.

Equation (5b) must be considered a rougher approximation than the other available methods, but it does provide a useful independent check. Unfortunately, the surface velocity exponent p is not known at this time for most saturated media. Both SGZ velocities and the exponent p have been accurately measured for saturated clay shale ($V_0 = 3.8 \times 10^5\ \text{dob}^{-1.5}$ for dob from 140 to 200 ft/kt$^{1/3}$, and $p \approx 2.5$). These values may apply to other saturated weak rock media as well. It is expected that p will fall between 2.1 and 3.0 for most saturated media.

All of the above methods normally give peak radial particle velocities and/or peak rock pressures as a function of scaled range. The results may also be expressed in terms of true range [true range = $(W^{1/3})$ (scaled range)] when they are applied to a specific experiment. It is often convenient to plot ΔP_{rock} as a function of true range or scaled range for a given experiment. This plot will take the form of two straight lines (inelastic and elastic regions) in a log-log graph.* The peak radial stress, ΔP_{rock}, in the cratering medium may be read directly from the graph.

Finally, it should be noted that all of the above methods apply only for a cratering medium identical to the medium for the two-layer experiment in question. If the cratering material under the water layer is saturated,† then the data used to derive U_{radial} and ΔP_{rock} must be for a similar saturated medium. This presents a particular problem for Methods (c) and (d), because the available data apply to experiments with no overlying water layer. Care must be exercised to select the data for a medium as close to the actual experimental conditions as possible (usually, a completely saturated medium).

---

*Refer to Appendix B for further discussion of shock pressures and particle velocities in the cratering medium.

†"Saturated" is defined as 90% or greater saturation (90% or more of the void volume in the material is filled with water).

Section 5. Predicting Range-Dependent Peak Water Surface Spall Velocities

Peak radial stresses in the cratering material will now be used to determine the transmitted peak pressures in the water layer and the resultant spall launch velocities. Necessary quantities are listed in Table 1 ($\rho_w C_w$), Table 2 (C_w), and Table 4 (C_r, U_r, $\rho_r C_r$, and $\rho_r U_r$ for various cratering media). Other sources may supplement Table 4 if better data are available. Record the appropriate constants for the test site in question at the top of Table 5. List the charge depth of burial in the cratering medium, D_r, and the depth of the overlying water layer, D_w, as well. Figure 1 shows the experiment configuration and the nomenclature used.

The transmitted peak pressures in the water layer and the corresponding water surface spall launch velocities, V(water), must be calculated for several surface locations. Table 5 provides a convenient format for tabulating all calculations. First, the angle at which the direction of shock propagation in the rock or cratering layer intersects the rock-water interface must be specified. This angle is called θ_r. When the shock wave crosses the rock-water interface, it is refracted and propagates away from the interface at a new angle θ_w. The angle θ_w may be determined from the law of refraction—Eq. (7), below. After determining θ_r and θ_w, it is possible to calculate the propagation slant ranges in the rock layer, S_r, and in the water layer, S_w. With S_r and the results of Section 4, it is then possible to compute the peak radial stress, ΔP_{rock} (at S_r), on the rock side of the rock-water interface. Finally, the pressure transmission factor $T(\theta_r)$ at the interface is calculated, and the pressure transmission through the water layer is determined. The water pressure, in turn, controls the spall launch velocity of the water surface. The equations for calculating all of these quantities are discussed below.

It is first necessary to calculate the shock pressures and the spall launch velocity in the vertical direction, at SGZ. For the vertical direction, $\theta_r = 90°$ (see the vertical ray shown in Fig. 1). Because the vertical ray suffers no refraction at the interface, $\theta_w = \theta_r = 90°$. The first line of Table 5 contains spaces for the $\theta_r = 90°$ calculations. The last column has a space for V_0 (water), the peak vertical spall velocity at SGZ. The subsequent lines of Table 5 are used for recording calculations at other θ_r values ($\theta_r = 80°$, 70°, 60°, etc.). A peak vertical spall velocity, V(water), must be calculated for each of these θ_r values. The final result of these calculations will be a complete spall velocity profile, encompassing a broad range of distances moving away from SGZ.

The detailed procedures and equations for calculating the quantities in Table 5 are as follows:

First, specify the angle at which the direction of shock propagation in the rock layer intersects the rock-water interface, θ_r. Use θ_r to determine the propagation slant range, S_r, in the rock layer:

$$S_r = \frac{D_r}{\sin \theta_r}. \qquad (6)$$

Table 5. Calculation of peak water surface spall velocities as a function of surface range from SGZ.

$\rho_r C_r$ = psi-sec/ft C_r = ft/sec $\rho_w C_w$ = psi-sec/ft C_w = ft/sec

$\rho_r U_r$ = psi-sec/ft U_r = ft/sec

D_r = ft D_w = ft

θ_r (°)	S_r (ft/kt$^{1/3}$)	θ_w (°)	S_w (ft/kt$^{1/3}$)	ΔP_{rock} (at S_r) (psi)	$T(\theta_r)$	Surface range, R_w (ft/kt$^{1/3}$)	ΔP_{water} (at R_w) (psi)	Vertical velocity, V(water) (ft/sec)
90	$S_r = D_r$	90°	$S_w = D_w$		T(at θ_r = 90°)	0.0		V_0 (water) = at SGZ
80								
70								
60								
50								
40								
30								
25								
20								
15								
10								

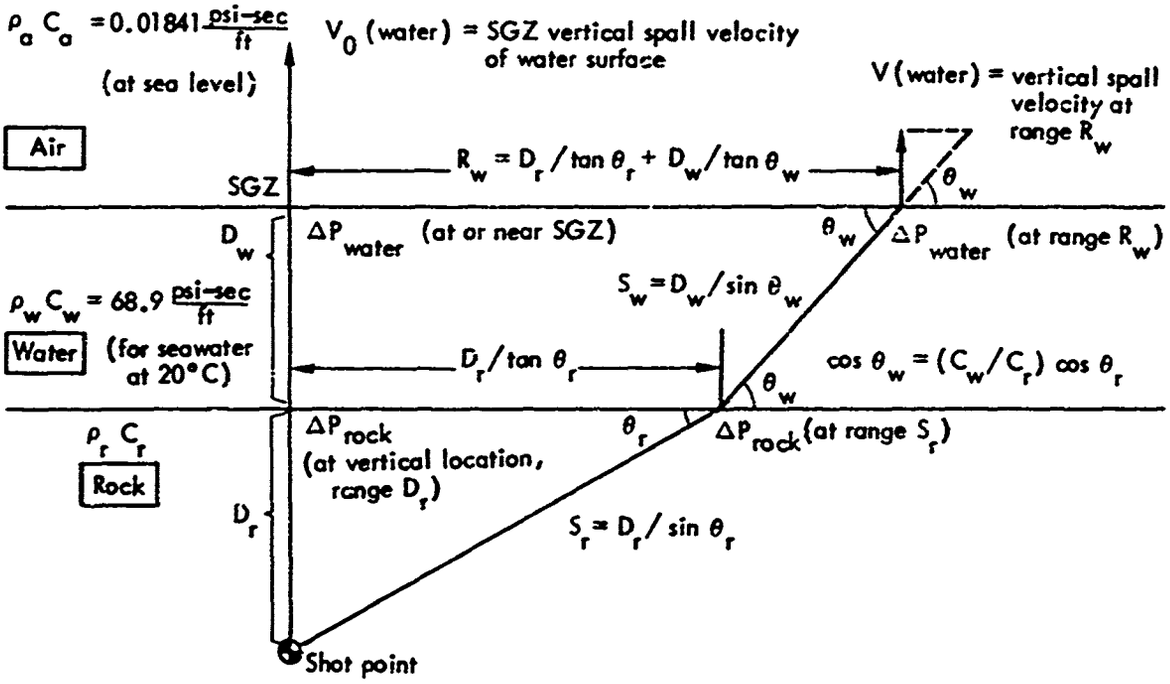

Fig. 1. Shock wave transmission for cratering medium overlain by water layer of small-to-moderate thickness ($D_w \approx D_r$).

Unless it is traveling in the vertical direction ($\theta_r = \theta_w = 90°$), the shock wave will be refracted upon crossing the interface; the angle θ_w at which the direction of propagation enters the water layer is given by the law of refraction:

$$\cos \theta_w = \cos \theta_r \frac{C_w}{U_r}. \qquad (7)^*$$

If the propagation range, S_r, is in the elastic region for the given calculation, substitute C_r for U_r in Eq. (7) (see Section 4). Calculate and record θ_w. Input data for this step may be obtained from Tables 2 and 4, or other sources.

Determine the propagation slant range, S_w, through the water layer:

$$S_w = \frac{D_w}{\sin \theta_w}. \qquad (8)$$

Using the results of Section 4, find the peak radial stress, ΔP_{rock} (at S_r), on the rock side of the rock-water interface. Record ΔP_{rock} (at S_r) in the table.

*Subject to the condition that C_r/C_w or $U_r/C_w \geq 1.0$. From Huygen's principle, the law of refraction [Eq. (7)] applies if $\cos \theta_r \leq C_r/C_w$ or U_r/C_w, which is always true if the velocity ratio is greater than 1.

Next, calculate the pressure transmission factor at the rock-water interface, T, which may be expressed as $T(\theta_r)$ for a specified set of input parameters. The value of $T(\theta_r)$ (ignoring shear in the cratering medium and considering only the stress wave*) is given by:

$$T(\theta_r) = \frac{2\,\rho_w C_w \cos(90^\circ - \theta_r)}{\rho_w C_w \cos(90 - \theta_r) + \rho_r U_r \cos(90 - \theta_w)} \quad (9)^\dagger$$

Table 6. Acoustic impedance, $\rho_r C_r$, for typical underwater cratering media.[7]

Medium	$\rho_r C_r$ (psi-sec/ft)
Silicon sand	144
Coral sand	118
Sea sand[a]	214
Coral	136-206
Granite	734
Rock (cement)	374

[a]Vineyard sound.

where the angle θ_w is obtained from Eq. (7), above. If the propagation range S_r is in the elastic region, substitute $\rho_r C_r$ for $\rho_r U_r$ in Eq. (9), as usual. Typical values of $\rho_r U_r$ and $\rho_r C_r$ are given in Table 4, while values of $\rho_r C_r$ for additional underwater cratering media are listed in Table 6. Table 1 summarizes $\rho_w C_w$ values.

Next, calculate the water surface range from SGZ, R_w, at which the shock wave reaches the water surface (see Fig. 1):

$$R_w = \frac{D_r}{\tan\theta_r} + \frac{D_w}{\tan\theta_w}\,; \quad (10)$$

R_w obviously approaches zero for $\theta_r = 90°$ (vertical ray).

Determine the peak pressure in the water layer at R_w, where the shock wave reaches the water-air interface[9,11,15]:

$$\Delta P_{water}\ (\text{at surface range } R_w) \cong$$

$$T(\text{at } \theta_r)\,\Delta P_{rock}\ (\text{at } S_r)\left[\frac{D_r}{R_w^{1/2}}\left\{\frac{\tan(90^\circ - \theta_r)}{D_r + D_w\dfrac{\tan(90 - \theta_w)[1 + \tan^2(90 - \theta_w)]}{\tan(90 - \theta_r)[1 + \tan^2(90 - \theta_r)]}}\right\}^{1/2}\right]^{1.13} . \quad (11a)^{**}$$

*Shear pulses are almost always negligible for completely saturated media, which have Poisson ratios close to 1/2, similar to a perfect fluid.

†This and subsequent equations use an acoustic approximation and the local sonic velocity, C_w, for water. However, it can be shown[1] that the shock front velocity is nearly equal to C_w and that the acoustic equations apply in most cases of interest for water shock pressures $\Delta P_{water} < 20{,}000$ psi.

**Refer to discussion in Appendix A.

For the special case of $\theta_r = 90°$ (vertical direction), this equation reduces to:

$$\Delta P_{water} \text{ (at surface range } R_w = 0) \cong$$

$$T(\text{at } \theta_r = 90°)\, \Delta P_{rock} \text{ (at } D_r) \left[\frac{D_r}{D_r + (C_w/U_r)(D_w)}\right]^{1.13} . \qquad (11b)$$

If the propagation range (D_r in this case) is in the elastic region, substitute C_r for U_r in Eq. (11b).

Finally, the peak vertical spall velocity, V(water), at surface range R_w is given by:

$$V(\text{water}) = \frac{2\, \Delta P_{water} \text{ (at surface range } R_w)}{\rho_w C_w} \sin \theta_w . \qquad (12a)$$

For the special case of $\theta_r = 90°$, this equation reduces to:

$$V_0(\text{water}) = \frac{2\, \Delta P_{water} \text{ (at surface range } R_w = 0)}{\rho_w C_w} \qquad (12b)$$

where V_0(water) is the peak vertical spall velocity at SGZ.

Perform the above calculations for each θ_r listed in Table 5; record the calculated R_w and V(water) values in each case.

Section 6. Predicting Water-Shock-Induced Airblast Overpressures

The peak vertical spall velocity profile is a vertical cross section of the detonation velocity mound taken through SGZ. Given the velocities calculated in the previous section, it is possible to plot the spall velocity profile and to predict far-field water-shock-induced airblast overpressures. The far-field overpressures at surface level are assumed to attenuate acoustically, as $R_w^{-1.0}$. The approximate value of the source strength constant in the acoustic equation is obtained by Montan's method,[4,5] which estimates the relative source strength by using the SGZ spall velocity V_0 and the integral of the spall velocity profile. It is first necessary to integrate the peak spall velocity profile graphically. On linear graph paper, plot the peak surface spall velocities, V(water), determined in Section 5, as a function of surface range, R_w, from SGZ; V(water) is usually expressed in ft/sec, and R_w in feet, while SGZ is located at $R_w = 0.0$. The highest velocity is, of course, V_0(water) at SGZ. Plot all other V(water) points symmetrically on both sides of SGZ (in other words, the range of integration for R_w extends from $-\infty$ to $+\infty$; the gradually decreasing velocity profile extends symmetrically away from SGZ on both sides). Draw a smooth curve through the plotted

V(water) points. This curve is the surface velocity profile. Integrate graphically* to obtain the integral:

$$\int_{-\infty}^{+\infty} V(\text{water})\, dR_w \qquad \text{(expressed in } ft^2/sec\text{)}$$

In reality, the extreme outer wings of the velocity profile have very little effect on the integration and may be ignored. Therefore, the integral is taken over some reasonable interval, $-R'_w$ to $+R'_w$, such that the important central part of the velocity field is included:

$$\int_{-R'_w}^{+R'_w} V(\text{water})\, dR_w \cong \int_{-\infty}^{\infty} V(\text{water})\, dR_w \,.$$

Substitute the value of the velocity profile integral into Eq. (13) and calculate "α," which is a dimensionless constant for a given detonation:

$$\alpha = \frac{1}{2\pi\,(D_r + D_w)\,V_0\,(\text{water})} \int_{-\infty}^{+\infty} V(\text{water})\, dR_w . \tag{13}$$

Next, calculate the local or near-field airblast overpressure at SGZ, ΔP_0:

$$\Delta P_0 = \frac{P_{ambient}}{P_{STP}} (\rho_a C_a)\, MV_0\,(\text{water}) \tag{14}$$

where

$P_{ambient}$ = ambient air pressure at SGZ for the given experiment (may be determined from meteorological data or from the altitude of the experiment location).

P_{STP} = ambient air pressure at standard sea-level conditions; P_{STP} = 1013 mbar = 14.68 psi.

$\rho_a C_a$ = acoustic impedance of air under standard sea-level conditions; $\rho_a C_a \cong 0.01841$ psi-sec/ft.

V_0 (water) = peak vertical spall velocity at SGZ (in ft/sec);

M = Mach number of the air shock at SGZ—Eq. (15); M ≈ 1.0 for small surface spall velocities.

If the above units are used for $\rho_a C_a$ and V_0 (water), then ΔP_0 will be in psi.

The Mach number of the air shock at SGZ is determined from the equation:

$$M^2 - \frac{\gamma + 1}{2} \frac{V_0\,(\text{water})}{C_a} M - 1 = 0 , \tag{15}$$

*The integral is considered to be positive on both sides of $R_w = 0$; in other words, the total integral is twice the value of the profile integral from $R_w = 0$ to $R_w = \infty$.

where $\gamma \cong 1.4$ (for air or any ideal gas) and C_a is the undisturbed sonic velocity in air at sea level; $C_a \cong 1087$ ft/sec. Technically, the true local sonic velocity, C_a (local), should be used instead, but C_a (local) $\approx$ 1087 ft/sec for most cases of interest.

Equation (15) is rather tedious to solve by hand; the solution is plotted as a function of (V_0/C_a) in Ref. 5.

The constants ΔP_0 and α calculated above are used to predict the far-field airblast overpressure, ΔP, as a function of surface range, R_w:

$$\Delta P \text{ (at range } R_w) = \Delta P_0 \, \alpha \left(\frac{D_r + D_w}{R_w} \right) . \qquad \Delta P \text{ and } \Delta P_0 \text{ in psi.} \qquad (16)^*$$

Equation (16) applies only to overpressures at or just above the water surface level, and only to far-field overpressures at ranges beyond the region of appreciable water surface spall motion. The far-field for broad velocity profiles of the type in question here[5] is normally defined by:

$$\frac{R_w}{D_r + D_w} \gtrapprox 2 . \qquad (17)$$

Predict the overpressures, ΔP, at several far-field ranges, R_w. Plot the resultant points on log-log graph paper and connect them with a straight line. The line has a slope of $R_w^{-1.0}$ and may be used to predict airblast at any far-field range closer than the region of appreciable meteorological effects (several miles from SGZ for large-yield events; slightly closer for small yields).

At near-field ranges (inside the region of appreciable water surface spall motion), the overpressure pulses from various parts of the rising water surface do not have an opportunity to combine. Therefore, the uncombined or local spall-induced overpressure is a quantity of interest. The local overpressure at any near-field location is given by:

$$\Delta P_{local} \text{ (at range } R_w) = \frac{P_{ambient}}{P_{STP}} (\rho_a C_a) \, MV(\text{water, at range } R_w), \qquad (18)$$

where M is a function of the local velocity ratio, V(water)/C_a—refer to Eq. (15). Equation (18) applies only for locations at or just above the water surface level, and only for near-field ranges $(R_w/D_r + D_w) < 1$ to 2. The local overpressure at SGZ, ΔP_0, has already been calculated—Eq. (14). Local overpressures at all other ranges should be correctly predicted by Eq. (18). However, some combination and reinforcement of overpressure pulses can occur even at near-field ranges. For this reason, ΔP_0 may be used as a safe-sided estimate of the true peak overpressure anywhere in the near-field.

*More correctly, one should use apparent charge depth, D_{ap}, (allowing for refraction of the wavefront) rather than the true depth $(D_r + D_w)$ in this equation. However, terms involving D_{ap} cancel between Eqs. (13) and (16), allowing the use of any desired depth normalization (see Appendix C).

The above airblast predictions apply to locations at or a few feet above the water surface. An approximate technique developed by Montan is sometimes used to predict far-field overpressures at greater elevations.[4] Consider a location at height, h, above the water surface (Fig. 2). Drop a perpendicular from this location to the water surface. The perpendicular intersects the water at a surface range R_w from SGZ. Draw a line from SGZ to the elevated location. The length of this line is the true range:

$$\text{True range} = \left(R_w^2 + h^2\right)^{1/2}. \qquad (19)$$

The line intersects the perpendicular at an angle "$\theta_{elevation}$" given by

$$\cos\,\theta_{elevation} = h \Big/ \left(R_w^2 + h^2\right)^{1/2}. \qquad (20)$$

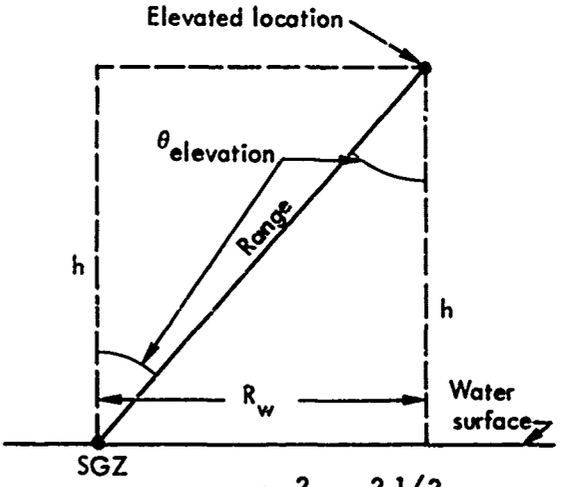

$\cos\,\theta_{elevation} = h/(h^2 + R_w^2)^{1/2}$

$= h/(\text{range to elevated location})$

Fig. 2. Elevated airblast (above water surface level).

The peak overpressure at the elevated location, $\Delta P_{elevated}$, is then[4]:

$$\Delta P_{elevated}\left[\text{at range } \left(R_w^2 + h^2\right)^{1/2}\right] = \Delta P_0\, \alpha \left[\frac{D_r + D_w}{\left(R_w^2 + h^2\right)^{1/2}}\right] \frac{1}{\cos\,(90° - \theta_{elevation})}. \qquad (21)$$

Equation (21) is valid only for far-field ranges $\left[\left(R_w^2 + h^2\right)^{1/2}/(D_r + D_w)\right] \gtrsim 2$, and only for angles $\theta_{elevation} > 15°$. Even within this region, the equation is not rigorously correct. Its use is justified primarily by the fact that it produces accurate overpressure predictions for intermediate far-field ranges and angles $\theta_{elevation}$ not extremely close to the vertical.[5] Rigorous derivation of the far-field elevated overpressures would require a complete knowledge of the velocity-time history of the entire water surface spall. Such information is not available for the complex multiple-layer cases under discussion here.

Section 7. Sample Problem

Perhaps the most interesting case for applied airblast predictions is saturated high-strength rock overlain by water. The acoustic impedance and shock transmission

properties of the cratering medium differ greatly from those of water in this case. Appropriate input data for most saturated high-strength media are somewhat lacking. However, the shock transmission properties of saturated andesite have been extensively studied. The available data derive from nuclear experiments, but may be provisionally applied to all types of events until better information is obtained.

Observations of nuclear tests in saturated andesite have shown that the free-field peak radial particle velocities fit empirical relations of the form[6]:

Inelastic region, $R_s < 580$ ft/kt$^{1/3}$: $U_{radial} = 7.81 \times 10^5 R_s^{-1.8}$,

Elastic region, $R_s > 580$ ft/kt$^{1/3}$: $U_{radial} = 4.70 \times 10^3 R_s^{-1.0}$,

where R_s is the scaled range from shot point in ft/kt$^{1/3}$.

The acoustic impedances and the peak radial stress wave and sonic wave velocities for saturated andesite are listed in Table 4:

Inelastic region: $\rho_r U_r = 300$ psi-sec/ft, $U_r = 9500$ ft/sec.

Elastic region: $\rho_r C_r = 395$ psi-sec/ft, $C_r = 12{,}500$ ft/sec.

The above information is substituted into Eqs. (2) and (3), giving the peak stresses in the rock layer:

Inelastic region: $R_s < 580$ ft/kt$^{1/3}$: $\Delta P_{rock} = 2.342 \times 10^8 R_s^{-1.8}$,

Elastic region: $R_s > 580$ ft/kt$^{1/3}$: $\Delta P_{rock} = 1.856 \times 10^6 R_s^{-1.0}$,

where ΔP_{rock} is the peak radial stress (psi). The acoustic impedance and sonic velocity in the overlying water layer are assumed to be:

Water: $\rho_w C_w = 68.96$ psi-sec/ft, $C_w = 4994$ ft/sec (see Tables 1 and 2, seawater at 20°C).

These data may be used to calculate peak water surface spall velocities by the method discussed in Section 5. The ΔP_{rock} equations are expressed in units of scaled range (ft/kt$^{1/3}$); therefore, it is convenient to use scaled distance units throughout the prediction calculations. This procedure does not limit the applicability of the results, since the predicted ΔP_0 and α values will apply to all detonations at the same scaled rock and water depth. Only the distance units in the final airblast prediction—see Eqs. (16) or (21)—will change for events that differ from 1 kt in yield.

As a sample problem, a typical prediction calculation has been performed for rock depth $D_r = 200$ ft/kt$^{1/3}$, and overlying water depth $D_w = 60$ ft/kt$^{1/3}$. The results of this calculation, extending to a water surface range of 771 ft/kt$^{1/3}$ from SGZ, are shown in Table 7. Note that all dimensions listed in the body of the table are scaled (ft/kt$^{1/3}$). The predicted peak vertical spall velocities of the water surface are given in the last column of the table. The (maximum) velocity at SGZ is V_0 (water) = 155.3 ft/sec. The velocity profile may be integrated, as discussed in Section 6, to give α. Velocities from Table 7 may be plotted on linear graph paper as a function of surface range R_w from SGZ (profile plotted symmetrically, on both sides of SGZ). The area under the resultant curve may then be integrated graphically to some reasonable range from

Table 7. Sample problem. Calculation of peak water surface spall velocities as a function of surface range from SGZ.[a]

$\rho_r C_r$ = 395 psi-sec/ft C_r = 12,500 ft/sec $\rho_w C_w$ = 68.96 psi-sec/ft C_w = 4994 ft/sec

$\rho_r U_r$ = 300 psi-sec/ft U_r = 9,500 ft/sec D_w = 60 ft/kt$^{1/3}$

D_r = 200 ft/kt$^{1/3}$

θ_r (°)	S_r[b] (ft/kt$^{1/3}$)	θ_w (°)	S_w (ft/kt$^{1/3}$)	ΔP_{rock} (at S_r) (psi)	$T(\theta_r)$	Surface range, R_w (ft/kt$^{1/3}$)	ΔP_{water} (at R_w) (psi)	Vertical velocity, V(water) (ft/sec)
90	$S_r = D_r$ = 200	90	$S_w = D_w$ = 60	16,900	$T(\theta_r = 90)$ = 0.374	0.0	5350	V_0 (water) = 155.3 ft/sec at SGZ
80	203	84.8	60.3	16,400	0.371	40.8	5180	149.6
70	213	79.6	61	15,100	0.360	83.8	4670	133.3
60	231	74.8	62	13,050	0.342	132	3900	109.0
50	261	70.3	64	10,460	0.316	189	2940	80.3
40	312	66.3	65	7,630	0.278	265	1940	51.5
30	400	62.9	67	4,850	0.228	377	1040	26.9
25	473	61.5	68	3,590	0.198	461	680	17.3
20	585[c]	67.9	65	3,170	0.121	574	374	10.0
15	772	67.3	65	2,400	0.0936	771	220	5.88
10	—	—	—	—	—	—	—	Negligible

[a]Example calculated for scaled ranges, in ft/kt$^{1/3}$; will also be used for a sample yield of 0.005 kt—see text.

[b]All ranges listed in this table are expressed in scaled units; thus, the slant range, S_r, is equivalent to the scaled range, R_S (ft/kt$^{1/3}$), used in the text.

[c]Elastic region of propagation in the rock layer begins; transition range = 580 ft/kt$^{1/3}$.

SGZ (to R_w = 771 ft/kt$^{1/3}$ on each side of SGZ in this case). The profile integral is used to determine α.

$$\int_{R_w=-771\ ft/kt^{1/3}}^{R_w=+771\ ft/kt^{1/3}} V(water)\, dR_w = 75{,}230 \text{ scaled ft}^2/\text{sec (by graphical integration)}$$

$$\alpha = \frac{1}{2\pi(D_r + D_w)\, V_0\ (water)} \int V(water)\, dR_w = \frac{1}{2\pi(260)\ (155.3)}\ (75{,}230) = 0.297.$$

The local airblast overpressure ΔP_0 at SGZ may also be calculated—Eq. (14). First, assume an ambient air pressure of $P_{ambient}$ = 1013 mbar (sea level). The acoustic impedance of air is $\rho_a C_a \cong 0.01841$ psi-sec/ft. The Mach number M, as determined from Eq. (15), is M = 1.089. The local overpressure ΔP_0 is then $\Delta P_0 = (P_{ambient}/P_{STP})\ (\rho_a C_a) M V_0$ (water) = 3.11 psi. This result may be corrected to any other ambient air pressure by substituting the appropriate value for $P_{ambient}$.

It is now possible to apply Eq. (16) and to predict the far-field airblast overpressures ΔP:

$$\Delta P = \Delta P_0\, \alpha \left(\frac{D_r + D_w}{R_w}\right) = 3.11\ (0.297) \left(\frac{200 + 60}{R_w}\right) = \frac{240}{R_w}\ ,$$

where ΔP is expressed in psi, and R_w is in scaled units, ft/kt$^{1/3}$. Note that the above equation applies to locations at or near water surface level, and for far-field ranges $(R_w/D_r + D_w) \gtrsim 2$, or $R_w \gtrsim 520$ ft/kt$^{1/3}$. Overpressures at elevated locations may be predicted using Eq. (21), subject to the limitations stated in Section 6.

The scaled predictions above may be easily adapted for any desired explosive yield. As an example, perform an airblast prediction for a 5-ton (0.005-kt) equivalent yield chemical explosive charge under the conditions of the sample problem (change scaled dimensions to true dimensions):

$$D_r = 200\ ft/kt^{1/3} = 34\ ft,$$

$$D_w = 60\ ft/kt^{1/3} = 10\ ft,$$

and, from Eq. (16),

$$\Delta P = \Delta P_0\, \alpha \left(\frac{D_r + D_w}{R_w}\right) = 3.11\ (0.297) \left(\frac{34 + 10}{R_w}\right)$$

$$\Delta P = \frac{40.6}{R_w} \text{ where } R_w \text{ is in true (instead of scaled) feet.}$$

The prediction is valid near water surface level and for ranges $R_w \gtrsim 88$ ft.

Note that all airblast predictions in this report are based on "acoustic" or $R^{-1.0}$ overpressure attenuation. Effects such as deviation from acoustic behavior (strong shocks), nonsymmetric shock propagation, and atmospheric temperature gradient may cause the attenuation rate to vary. The wide changes in observed attenuation rates for similar experiments indicate that local effects (rather than nonacoustic shock effects) are responsible for deviations from $R^{-1.0}$ attenuation. Temperature gradient is the most important local factor influencing far-field airblast. At locations near the ocean, the lower layers of air typically show a strong temperature gradient; such conditions cause sound to be refracted upwards, away from the surface level. Thus, the overpressure pulse is expected to attenuate somewhat more rapidly than $R_w^{-1.0}$ at surface level. If a strong gradient prevails, the overpressure predictions may be slightly improved by attaching a line of slope $R_w^{-1.2}$ to the normal $R_w^{-1.0}$ line at "long" ranges, beyond the region of close-in acoustic attenuation [very roughly, attach an $R_w^{-1.2}$ line at ranges greater than $R_w \approx 10$ to 20 times $(D_r + D_w)$]. This procedure gives an approximation of the faster attenuation and lower overpressures at ranges beyond the close-in region.

It should also be noted that the opposite atmospheric effect of a temperature inversion* can cause refraction of sound waves toward ground level, with resultant focusing. Under these conditions, overpressures may attenuate more slowly than $R_w^{-1.0}$, producing increased airblast at long ranges (≈ a few miles from SGZ) where the focusing is most likely to occur. Other atmospheric effects may focus sound waves at very long ranges, but these effects become important only for large multi-kiloton detonations capable of creating damage at such extreme ranges

Section 8. Summary

A method is presented for estimating water-shock-induced airblast from single-charge cratering detonations in saturated media overlain with water. The method requires as input data a knowledge of the acoustic impedances and sonic velocities in the cratering medium and water layers, as well as an empirical fit to the shock propagation parameters in the cratering medium. Predictions made using this technique have not yet been adequately compared with actual airblast data, and future observations may reveal the need for some improvements. To verify and to extend the method, measurements of airblast and time-dependent water surface spall velocity for an underwater cratering event in intermediate- or high-strength rock are needed.

The procedures described in this report are easily adapted for computer use. A relatively simple code may be written to calculate peak water surface spall velocities as a function of range R_w, over small intervals in R_w (or over small increments of θ_r).

*Temperature increases with altitude in the near-surface layers.

The resultant velocity profile may be integrated numerically to some reasonable outer limit in R_w or V(water),* giving the value of α. Computer calculations provide a particularly convenient means of calculating ΔP_0 and α for a number of different rock and water depth combinations in a variety of media. A computer program that calculates ΔP_0 and α for depth combinations $20 \leqq D_w \leqq 320$ ft/kt$^{1/3}$ and $60 \leqq D_r \leqq 320$ ft/kt$^{1/3}$ is presented in Appendix B. Some sample problems solved using this program are discussed.

*A reasonable criterion for limiting the calculation might be $R_w \approx 5(D_r + D_w)$, or V(water) $\approx 0.02\ V_0$(water).

Appendix A
Pulse Transmission in the Water Layer

Appendix A
Pulse Transmission in the Water Layer

An approximation that describes the elastic propagation of refracted acoustic compression waves in two-layered media has been developed by Hipp, Gerjouy, Horton, and others.[11,15] This approximation, derived from fundamental considerations of geometry and energy conservation, allows for spherical aberration and astigmatism of the wavefront in the second medium. It does not allow for curvature of the wavefront or nonacoustic pressure attenuation. With the insertion of a small correction for attenuation, the Hipp-Gerjouy-Horton treatment is used in this report. Complete derivations may be found in the literature, but the equations are summarized here for the reader's convenience.

Assume that the second layer consists of water, and let ΔP_{wi} be the peak water pressure caused by a given ray at the rock-water interface. Then ΔP_{wi} may be calculated from Eq. (9):

$$\Delta P_{wi} = T(\theta_r)\, \Delta P_{rock}\ (\text{at } S_r)\ ,$$

where

$T(\theta_r)$ = acoustic transmission factor at the rock-water interface

ΔP_{rock} (at S_r) = rock pressure at the rock-water interface.

The refracted compression wave, ΔP_{wi}, will continue to propagate through the water layer, reaching the surface at surface range, R_w, from SGZ. The water pressure at the surface, ΔP_{water} (at surface range R_w), is then given by:

$$\Delta P_{water}\ (\text{at surface range } R_w) \cong \Delta P_{wi} \left[\frac{D_r}{R_w^{1/2}} \times \left\{ \frac{\tan(90° - \theta_r)}{D_r + D_w \dfrac{\tan(90 - \theta_w)[1 + \tan^2(90 - \theta_w)]}{\tan(90 - \theta_r)[1 + \tan^2(90 - \theta_r)]}} \right\}^{1/2} \right] A\ .$$

The A-term is a correction factor that allows for nonacoustic pressure attenuation in the second layer; $A \approx 1.13$ for water. The above equation is in turn used to derive Eq. (11) of the text.

Appendix B

MULTIMEDIA-Computer Calculation of Two-Layer Airblast Parameters

Appendix B
MULTIMEDIA—Computer Calculation of Two-Layer Airblast Parameters

MULTIMEDIA is a computer program (code) that utilizes the method discussed in the foregoing report to calculate the peak vertical spall velocity profile of the water surface above detonations in two-layered media (cratering medium overlain by water), to integrate the velocity profile, and to determine α and ΔP_0. The quantities α and ΔP_0 may then be used to predict peak airblast overpressures, ΔP, as described in Section 6.

The code calculates necessary shock wave propagation parameters for waves intersecting the rock-water interface at 1° intervals, starting with $\theta_r = 89°$ ($\theta_r = 89°$, 88°, 87°, 86°, ...). The calculated shock wave parameters at $\theta_r = 89°$ are used to approximate the water pressure and the peak vertical water surface spall velocity V_0 (water) at SGZ. This approximation is adopted as a matter of simplicity and convenience in the computer code; it has no significant effect on the numerical accuracy of the results. The velocity, V_0, is in turn used to obtain the peak local airblast overpressure, ΔP_0 (in psi), at SGZ. The calculated shock wave parameters for other θ_r angles give the water surface spall velocities, V(water), as a function of surface range, R_w, from SGZ. The calculations are terminated when the peak vertical water surface spall velocity decreases below $\frac{1}{50}$th of V_0 (or when $\theta_r = 4°$, whichever occurs first). The velocity profile of the water surface is integrated to the termination point symmetrically on both sides of SGZ [the velocity V(water) at $\theta_r = 89°$ is again used as an estimate of V_0 (water) in the integration]. The integral of the velocity profile is then used to calculate the value of α—see Eq. (13) of the text.

A complete list of the code is included at the end of this appendix.*

INSTRUCTIONS

In order to use the code, it is necessary to know the acoustic impedance (in psi-sec/ft) and sonic velocity (in ft/sec) in the water layer, acoustic impedance and sonic velocity for both the inelastic and elastic regions of the cratering medium, the scaled range of transition between the inelastic and elastic regions, the peak radial particle velocities caused by the shock wave in the inelastic and elastic regions, and the ambient air pressure at the experiment location (in millibars). Determination of these input quantities is discussed in the text of this report. Read the data into the computer in the following format:

First data card: All eighty columns: in alphabetical and numerical characters, enter the name of the medium, ambient air pressure, and any other desired information.

*The MULTIMEDIA code is written in FORTRAN II and runs approximately 3 min on a CDC 6600 computer.

Second card: Enter the acoustic impedance (psi-sec/ft) of water in the first five columns (format F5.0), and the sonic velocity (ft/sec) in the water in the second five columns (F5.0).

Third card: Enter the acoustic impedance (psi-sec/ft) in the inelastic region of the cratering medium in the first five columns (F5.0), the stress wave velocity (ft/sec) in the inelastic region of the cratering medium in the next five columns (F5.0), the scaled range of transition between the inelastic and elastic regions (in $ft/kt^{1/3}$) in the next five columns (F5.0), the acoustic impedance in the elastic region in the next five columns (F5.0), and the sonic velocity in the elastic region in the next five columns (F5.0).

Fourth card: The peak radial particle velocities in the cratering medium due to the shock wave are fitted by two connected (log-log straight line) equations of the form:

$$\text{Inelastic region: } V_{particle} \text{ (in ft/sec)} = A_1 \text{ (scaled range)}^{B_1},$$

$$\text{Elastic region: } V_{particle} \text{ (in ft/sec)} = A_2 \text{ (scaled range)}^{B_2},$$

where "scaled range" is the distance from the charge center, expressed in $ft/kt^{1/3}$. In the first nine columns of the data card enter A_1 (format E9.0), in the next five columns enter B_1 (format F5.0), in the next five columns enter the scaled range of transition between the inelastic and elastic regions ($ft/kt^{1/3}$) (format F5.0), in the next nine columns enter A_2 (format E9.0), and in the next five columns enter B_2 (format F5.0).

Fifth card: Enter the ambient air pressure at the experiment location (millibars) in the first eight columns (format F8.2). The ambient pressure at sea level is usually assumed to be 1013.0 mbar. The ambient pressure at 5000 ft MSL is approximately 844.0 mbar.

CODE OUTPUT

The code output occurs in the following format: At the top of the first output page, all of the identifying information punched on the first input card is printed out. This information includes the medium name, ambient air pressure, and anything else appearing on the first data card. Beneath the identifying information, calculated shock wave parameters for the first combination of water and rock depth are printed out. The first depth combination consists of a water depth $D_w = 20$ $ft/kt^{1/3}$ and a rock depth $D_r = 60$ $ft/kt^{1/3}$. The parameters are given for 1° intervals in angle of intersection with the rock interface, beginning at $\theta_r = 89°$ (88°, 87°, ...). In the first column, the angle at which the direction of shock wave propagation intersects the rock side of the rock-water interface, θ_r, is given; in the next column, the angle at which the (refracted) shock wave enters the water layer, θ_w, is listed; in the third column, the surface range R_w ($ft/kt^{1/3}$ from SGZ) at which the shock wave reaches the water surface is

listed; in the fourth column, the peak rock pressure at the rock-water interface is given. The next two columns list the transmission factor into the water layer $T(\theta_r)$ and the peak water pressure at the water surface, ΔP_{water} (at R_w) (in psi). In the seventh column, the peak vertical spall velocity of the water surface (in ft/sec) is listed; the final column gives the cumulative velocity profile integral (in scaled ft^2/sec) to this surface range on both sides of SGZ. These shock wave parameters are calculated and printed until the peak vertical spall velocity decreases below 1/50th of the V_0 at SGZ. The calculation is then concluded, and the final results are printed two lines below: first, the scaled water depth and rock depth ($ft/kt^{1/3}$) are printed out, followed by the Mach number, M, of the air shock at SGZ, then the approximate peak vertical spall velocity, V_0, of the water surface at SGZ (ft/sec), the peak local airblast overpressure ΔP_0 at SGZ (psi), and finally the airblast alpha value α (dimensionless). The local overpressure at SGZ, ΔP_0, and the dimensionless constant, α, may be used to predict water-shock-induced airblast for the given combination of water depth and rock depth, as discussed in Section 6 of the paper.

Next, the calculated shock wave parameters for the second combination of water depth and rock depth are printed out. The rock depth is increased by 20 $ft/kt^{1/3}$ over the previous value in this case. The output format is exactly the same as above: first, the calculated shock wave parameters are given for 1-deg intervals in angle of intersection with the rock interface, starting at θ_r = 89°. The calculation is again concluded when the vertical spall velocity decreases below 1/50th of the V_0 at SGZ. Final results are printed two lines below (the given scaled water depth and rock depth, Mach number M, peak vertical spall velocity V_0 at SGZ, peak local overpressure ΔP_0 at SGZ, and the dimensionless constant α).

The rock depth is next increased by another 20 $ft/kt^{1/3}$, and results for this depth are printed out. In this fashion, the program continues to increase the rock depth at 20 $ft/kt^{1/3}$ intervals until a depth of 320 $ft/kt^{1/3}$ is reached. Complete output results are printed for each depth. After a depth of 320 $ft/kt^{1/3}$ is reached, the program returns the rock depth to its original (smallest) value of 60 $ft/kt^{1/3}$ and increases the water depth by 20 $ft/kt^{1/3}$. Complete calculations are performed for this new depth combination and output results are printed in the usual format. The rock depth is again varied at 20 $ft/kt^{1/3}$ intervals up to 320 $ft/kt^{1/3}$, and complete results are printed for each depth. Afterwards, the water depth is increased by yet another 20 $ft/kt^{1/3}$, and complete data are calculated and printed out for each rock depth. This process continues until the final water depth of 320 $ft/kt^{1/3}$ is reached. The last set of calculations and the last set of printed data output are for the deepest combination of rock and water depth (rock depth = 320 $ft/kt^{1/3}$ and water depth = 320 $ft/kt^{1/3}$).

For certain input parameters and certain combinations or rock and water depth, the physical discontinuity between inelastic and elastic propagation regions in the rock may cause the change in surface range, dR_w, to become negative over one angle interval. This angle interval always occurs for the ray at the slant range, S_r, where

the elastic region first begins. When a negative change of R_w is encountered, the program prints a warning immediately below the data for the angle θ_r where this change takes place. Such a warning will occur no more than once in the tabulated data for a given depth combination. The program uses an absolute value of dR_w to calculate the velocity profile integral contribution over this interval. Actually, the physical discontinuity has no significant numerical effect on the final results; thus, it may be ignored for the purposes of interest here.

Finally, after all the depth combinations have been fully calculated, the important prediction parameters ΔP_0 and α are summarized in a convenient table at the end of the program output. Horizontally at the top of this table, all the water depths (D_w = 20 to 320 ft/kt$^{1/3}$) are listed. Vertically at the left side, the rock depths (D_r = 60 to 320 ft/kt$^{1/3}$) are given. Within the table, ΔP_0 and α values for each depth combination are compiled. The ΔP_0 (in psi) for each depth combination is printed directly above the α value. To read a value from this table, enter at D_w on the top list, proceed down to D_r (listed at the left), and read the desired ΔP_0 (top number) and α (bottom number).

To perform overpressure predictions for any given case, select values of ΔP_0 and α for the set of data closest to the desired combination of rock depth and water depth. Use these values to predict water-shock-induced airblast. In some cases, it may be necessary to interpolate linearly for ΔP_0 and α between tabulated values at rock depths or water depths differing by 20 ft/kt$^{1/3}$.

SPECIAL CASES: MODIFICATIONS TO THE CODE AND PREDICTION PROCEDURES

The output of the MULTIMEDIA code or the code itself may be modified to allow for certain variations in the specified conditions. For example, the predicted SGZ local airblast overpressures ΔP_0 are based on the assumed input value of ambient air pressure, $P_{ambient}$ (input). (See the discussion of input data cards, above.) After running the program, it may become necessary to convert the calculated ΔP_0 values to new ΔP_0 values for a different ambient pressure, $P_{ambient}$ (new). Any ΔP_0 value calculated by the program may be approximately converted to a new ΔP_0 value according to the following formula:

$$\text{New } \Delta P_0 = \frac{P_{ambient\ (new)}}{P_{ambient\ (input)}} \Delta P_0 \text{ (calculated)}.$$

The α values are not changed by a new value of $P_{ambient}$.

Also, the water and rock depths and depth intervals for which quantities are calculated may be changed from the values specified in the program. Statements 28 and 32 control the water and rock depths, respectively. These are "DØ" statements that tell the program to perform calculations from a specified minimum value to a specified maximum value (for example: "DØ 27 JJ = 3, 16"; in this case, 3 is the

minimum value and 16 is the maximum value). The first or smallest depth for which calculations are performed is twenty times the minimum value; the last or greatest depth for which calculations are performed is twenty times the maximum value. To change the minimum depth, modify the first (minimum) value in the appropriate statement; to change the maximum depth, modify the second (maximum) value in the appropriate statement. Calculations will still be performed at 20 ft/kt$^{1/3}$ intervals between the minimum and maximum depths, as usual.* If the minimum rock depth is changed during this step (Statement 32), Statement 122 must also be changed to agree with the new minimum depth. Statement 122 says "DØ 704 JK = 3, JKMAX." The number "3" must be changed to 1/20th of the new minimum depth.†

Note that calculations performed by the code for very shallow depths may be inaccurate due to the high water surface velocities (V_0 approaches or exceeds the local sonic velocity in air). In addition, shallow explosions may produce very strong supersonic plume and gas-vent effects, and these effects may become dominant in causing far-field airblast.[12-16] Thus, the code output cannot be used to perform airblast predictions for very shallow scaled depths. It should also be noted that code calculations at extremely deep scaled depths of burst (total depth >> several hundred ft/kt$^{1/3}$) are meaningless for acoustic airblast predictions, because perfect acoustic reinforcement between pulses from various parts of the rising surface no longer occurs. The true far-field overpressures fall below predicted acoustic values, and local overpressures may become important for some safety considerations. This situation occurs, however, only for very deep events.

The sonic velocity in air assumed for MULTIMEDIA is C_a = 1087.0 ft/sec. This velocity is usually correct within about 5% for near sea level conditions. The sonic velocity does vary with temperature, and a more accurate value may be inserted if desired. Statement 80 controls the sonic velocity: "RATIØ = VØ/1087.0." To change the assumed velocity, substitute the correct value in the denominator of this equation. The velocity should be expressed in ft/sec.

In certain cases, there may be no clearly defined transition range between the inelastic and elastic shock propagation regimes, or the medium properties may not be sufficiently well known to permit the establishment of two separate regimes. Under these conditions, the assumed shock velocities, acoustic impedances, and/or shock transmission properties may be identical for both regions. However, it is still necessary to repeat the required input data twice on the appropriate input cards. Choose any arbitrary value for the transition range, and insert this value on input cards three and four. List the required input parameters twice on these two cards, for the arbitrary "inelastic" and "elastic" regions (even though these data are the same for both regions). Note that this procedure is intended primarily for special cases, and

*Statements 29 and 33 control the water and rock depth intervals between successive calculations (factor of 20). These intervals may also be modified if desired.

†Numbers specified in "DØ" statements must always be integers (no decimal).

may not produce accurate results if the input data are used for regions outside their range of applicability (i.e., low-amplitude long-range shock transmission parameters and long-range "acoustic" medium properties applied to the close-range inelastic region). Normally, the transition range used by the program should correspond rather closely to a physically real transition in the shock propagation properties of the medium.

Sometimes the known characteristics of shock propagation in the cratering medium may include the peak shock stress, ΔP_{rock}, instead of the peak particle velocity, $V_{particle}$. The stress is usually fitted by two empirical equations of the form "$\Delta P_{rock} = K$ (scaled range)^B," one each for the inelastic and elastic propagation regions. The code requires peak particle velocities rather than stresses. However, the empirical stress equations may be easily converted to particle velocity equations: divide the constant K by the appropriate acoustic impedance $\rho_r U_r$ or $\rho_r C_r$ in each region (inelastic and elastic). The new equations thus obtained will be the correct particle velocity equations to use in each region.* Two separate equations must, of course, be calculated (for the inelastic and elastic regions). The attenuation rates "B" in each region, and the scaled range of transition between inelastic and elastic regions, are identical for both stress and particle velocity.

One additional modification may be applied to the MULTIMEDIA code, either before or after it is run. The integral solutions for α sometimes converge rather slowly, giving rise to large values of α. These values may become a little unrealistic, particularly for events at great scaled depths, because of the very broad linear extent over which the surface velocity field is integrated. The code itself may be modified to terminate the integration sooner. Statement 102 specifies the termination criterion. The calculation may be terminated closer to SGZ (at a higher peak velocity) by decreasing the constant in this statement. For example: the original statement reads "VTEST = VØ - 50.0 X VEL." If it is desired to terminate the integral at a velocity value of 1/30th V_0 (instead of 1/50th V_0), the statement should be modified to read "VTEST = VØ - 30.0 X VEL." Alternatively, a completely different termination criterion may be established, using "VTEST" as the decision parameter (see Statement 103). Positive "VTEST" terminates the integral.

Termination of the velocity integral may also be accomplished after the program has been run. The data output for each calculation includes a complete list of the calculated parameters at 1° intervals, from $\theta_r = 89°$ to the termination velocity. The last two columns of this list give the Vertical Velocity (of the water surface) and the Cumulative Velocity Profile Integral (up to the listed velocity value). The final value of α, printed below the list, is determined for the entire integrated velocity profile. To terminate the integral at a higher velocity, select any desired termination

*The particle velocities given by the two equations at the transition range should be the same; if they are not, adjust the constants slightly as necessary.

velocity from the list. Read the Cumulative Velocity Profile Integral at this velocity (last column). Calculate a new value of α for this termination point:

$$\text{New } \alpha = \frac{1}{2\pi V_0 \text{ (scaled rock depth + scaled water depth)}} \times \text{(CUM. VEL. PROFILE INTEGRAL)},$$

where

V_0 = vertical velocity of the water surface at SGZ (ft/sec);
Scaled depths in $ft/kt^{1/3}$.

SAMPLE PROBLEMS

MULTIMEDIA was first tested by application to certain simplified problems with known answers, and by comparative manual calculations for selected problems that were more complex. The numerical results are sufficientiy accurate for current predictive purposes. The code was next applied to several sample media, using estimated shock wave transmission parameters for these media. The preliminary trial cases included saturated andesite (a high-strength rock with known shock wave transmission characteristics for nuclear detonations), saturated clay shale (a weak rock with known shock wave transmission characteristics for nitromethane detonations), saturated coral (a very weak medium that fails in crushing, with estimated shock wave transmission characteristics for aluminized ammonium nitrate slurry—AANS—detonations), and saturated basalt (a high-strength rock with estimated shock wave transmission characteristics for TNT). The shock wave transmission characteristics are most accurately applicable to the given explosive-medium combination in each case, but the results will serve temporarily for estimating airblast from all sorts of explosives in the listed media. Better approximations to the shock wave and medium characteristics may be used in the future, when more data from explosive tests and output from SOC-TENSOR* analyses become available. Input data for the various sample media are shown on a standard computer coding form (Fig. B1). The first set of data is for saturated andesite (nuclear events), the second set is for saturated clay shale (nitromethane), the third set is for saturated coral (AANS), and the fourth set is for saturated basalt (TNT). Input data for the saturated basalt case must be considered rough estimates at this time; thus, predictions made using these data may be somewhat less accurate than the other cases.

As an example of the input format, examine the list for saturated clay shale (second set of data). The first card gives the medium name and identification. The

*One- and two-dimensional hydrodynamic codes in use at the Lawrence Livermore Laboratory.[2]

PROGRAMMER _____ DATE _____

PROBLEM _____ EXT. _____ PAGE _____

FORTRAN

7600-84610

C = FOR COMMENT | STATEMENT NUMBER | CONT | FORTRAN STATEMENT

```
FOR SATURATED ANDESITE OVERLAIN BY SEAWATER, P(AMBIENT) =1013MB
6 8.964994.
3 00.095 00.580.0395.012500
   7.81E+05 -1.8580.0 4.70E+03 -1.0
   1013.00

FOR SATURATED CLAY SHALE OVERLAIN BY SEAWATER, P(AMBIENT)=1013MB
6 8.964994.
1 91.064 00.140.0191.064 00.
1.454E+06-1.8414 0.01.795E+05-1.42
   1013.00

FOR SATURATED VERY WEAK CORAL OVERLAIN BY SEAWATER, P(AMBIENT)=1013MB
6 8.964994.
*136.063 00.700.0136.063 00.
   6.45E+05 -1.7700.0 4.69E+04 -1.3
   1013.00

FOR SATURATED BASALT OVERLAIN BY SEAWATER, ESTIMATE P(AMBIENT)=1013MB
6 8.964994.
4 50.011 90.040 0.059 4.015 700
   2.80E+06 -2.1400.0 1.27E+04 -1.2
   1013.00
```

*A transition range of 700 ft/kt$^{1/3}$ corresponds approximately to the maximum range of observed crushing near the coral surface.

Fig. B-1. Standard computer coding form.

second card lists the properties of seawater (at 20°C, 35-ppt salinity for the sample problem):

Acoustic impedance = 68.96 psi-sec/ft

Sonic velocity = 4994 ft/sec.

The third card lists acoustic impedances and shock wave velocities in the cratering medium, as well as the transition range between inelastic and elastic propagation regimes:

Inelastic: Acoustic impedance = 191.0 psi-sec/ft

Velocity = 6400 ft/sec

Transition range = 140.0 ft/kt$^{1/3}$

Elastic: Acoustic impedance = 191.0 psi-sec/ft

Velocity = 6400 ft/sec

(These quantities do not differ significantly between the propagation regions for highly saturated clay shale at ranges greater than 80 to 90 ft/kt$^{1/3}$.)

The fourth card gives the constants in the empirical particle velocity equations (nitromethane in saturated clay shale, inelastic and elastic regions), as well as the transition range:

Inelastic: $V_{particle} = 1.454 \times 10^{6}$ (scaled range)$^{-1.84}$

Transition range = 140.0 ft/kt$^{1/3}$

Elastic: $V_{particle} = 1.795 \times 10^{5}$ (scaled range)$^{-1.42}$

The final card specifies the ambient air pressure in mbar:

$P_{ambient}$ = 1013.00 mbar

The above shock wave and medium parameters are based on SOC-TENSOR code calculations for chemical explosive cratering detonations near optimum depth of burial in saturated clay shale.[17] Code predictions provided accurate estimates of the true peak pressures at the shock front. These peak pressures were converted to peak particle velocities via division by the acoustic impedance ρC = 191.0. Two straight line segments were fitted through the peak particle velocities for use by MULTIMEDIA. These straight line segments accurately approximate all of the SOC-TENSOR data in the region 80 ft/kt$^{1/3}$ < scaled range < several hundred ft/kt$^{1/3}$. The accepted value of acoustic impedance, ρC = 191 psi-sec/ft, is also known to be valid for scaled ranges > 90 ft/kt$^{1/3}$. MULTIMEDIA simply converts the fitted particle velocities back to peak pressures for use during the calculations. This is currently the most accurate method for estimating shock pressures in the clay shale. It should be noted that the two fitted particle velocity line segments do not correspond exactly to inelastic and elastic propagation regimes in this case; they are the best empirical approximations to shock properties in "high" and "low" pressure regimes for a weak highly saturated medium. Correlation between the empirical propagation regimes and

the inelastic-elastic transition is generally much closer for high-strength media or for media that fail in crushing.

Data abstracted from the code output for the four sample problems are given in Tables B1 through B4 (sample of code output with labels added). The listed information includes ΔP_0 (psi) and α for each combination water and rock depth. The water depths ($ft/kt^{1/3}$) are listed horizontally at the top of the table, and rock depths ($ft/kt^{1/3}$) are listed vertically on the left side. For each depth combination, the program tabulates a value of ΔP_0 (psi; top number) and a value of α (dimensionless; bottom number). It is important to remember that the calculations may be somewhat in error (due to the high velocities involved) and that gas-vent airblast may become dominant for very shallow total depths (upper left corner of the tables). Final results for each medium may be read from the appropriate table. As an example, examine Table B1 (saturated high-strength andesite): at water depth = 60 $ft/kt^{1/3}$, rock depth = 200 $ft/kt^{1/3}$, ΔP_0 = 3.11 psi, α = 0.309. (This value of α differs slightly from the hand-calculated value in the Section 7 sample problem because the integral was carried only to R_w = 771 $ft/kt^{1/3}$ in the hand-calculated problem.) The values of ΔP_0 and α read from Tables B1 to B4 may be used to predict far-field water-shock-induced airblast overpressures.

Results in the third sample table are applicable to saturated coral, and may be compared with the Tugboat single-charge airblast measurements.[5,18] (The tabulated solutions are based on estimated shock transmission parameters for slurry explosive in coral.*) Tables B5 through B7 list the ranges and far-field overpressures, ΔP, for five Tugboat single-charge events. Theoretical α's and ΔP_0's interpolated from Table B3 are also given for each experiment. The observed values and theoretical predictions are compared in Figs. B2 through B4. Theoretical lines are shown as $R_w^{-1.0}$, and as $R_w^{-1.2}$ (extrapolated from $R_w/(D_r + D_w)$ = 20.0). The faster $R_w^{-1.2}$ overpressure attenuation is typical of temperature gradient conditions in sea air, which often cause sound to be refracted away from ground level, decreasing the observed overpressures. Agreement between measurements and the theoretical predictions is excellent at "close" far-field ranges ($R_w/(D_r + D_w) \approx 5$ to 30). At longer ranges, the far-field overpressures tend to attenuate as $R_w^{-1.2}$. The observed overpressures for Event Id fall somewhat below the predictions. This fact could indicate a slightly defective shock transmission model in the coral, or an unusually strong atmospheric temperature gradient causing rapid attenuation of overpressure at the time of the shot.

Saturated coral as a shock transmitting medium does not vary too dramatically from pure seawater; therefore, the above results do not provide definitive support for the method. Airblast measurements for a single-charge event in a saturated high-strength medium overlain by water are urgently needed in order to make further improvements in predictive capability. The necessary data should include observations

*The estimated shock wave parameters were derived from theoretical considerations. Explosive properties for aluminized ammonium nitrate slurry were used in the derivation.

Table B1. ΔP_0 and α for nuclear explosives in saturated andesite (high-strength rock) overlain by seawater ($P_{ambient}$ = 1013 mbar).

Entries in pairs: ΔP_0—in psi, listed above; α—dimensionless, listed below.

SUMMARY OF DELTA P(0) AND ALPHA VALUES

WATER DEPTHS-FT/KT1/3) LISTED HORIZONTALLY ACROSS TOP

ROCK DEPTHS- FT/KT1/3)LISTED VERTICALLY

20.0	40.0	60.0	80.0	100.0	120.0	140.0	160.0	180.0	200.0	220.0	240.0	260.0	280.0	300.0	320.0
60.0															
48.52	37.96	30.84	25.79	22.04	19.17	16.92	15.11	13.62	12.38	11.34	10.45	9.68	9.01	8.42	7.90
0.298	0.272	0.255	0.243	0.234	0.226	0.220	0.216	0.211	0.208	0.204	0.201	0.200	0.197	0.195	0.194
80.0															
25.77	19.99	17.17	15.01	13.29	11.91	10.77	9.82	9.02	8.33	7.73	7.21	6.75	6.34	5.97	5.65
0.307	0.291	0.267	0.255	0.245	0.237	0.232	0.226	0.221	0.217	0.214	0.211	0.209	0.206	0.204	0.201
100.0															
14.29	12.52	11.12	9.99	9.05	8.26	7.60	7.02	6.53	6.09	5.71	5.37	5.07	4.79	4.55	4.32
0.311	0.292	0.276	0.265	0.255	0.247	0.240	0.234	0.231	0.226	0.222	0.219	0.216	0.213	0.210	0.208
120.0															
9.67	8.69	7.88	7.21	6.63	6.14	5.71	5.33	5.00	4.70	4.44	4.20	3.99	3.79	3.62	3.45
0.315	0.298	0.284	0.272	0.263	0.255	0.248	0.243	0.238	0.233	0.229	0.227	0.223	0.220	0.217	0.215
140.0															
7.04	6.41	5.93	5.49	5.11	4.77	4.48	4.22	3.98	3.77	3.58	3.40	3.24	3.10	2.97	2.84
0.320	0.303	0.289	0.280	0.270	0.262	0.257	0.250	0.245	0.240	0.237	0.234	0.230	0.227	0.224	0.223
160.0															
5.39	5.00	4.65	4.35	4.08	3.84	3.63	3.43	3.26	3.10	2.96	2.83	2.70	2.59	2.49	2.39
0.323	0.309	0.296	0.286	0.278	0.270	0.263	0.257	0.253	0.248	0.244	0.240	0.237	0.234	0.233	0.230
180.0															
4.29	4.01	3.76	3.54	3.34	3.17	3.01	2.86	2.73	2.61	2.50	2.39	2.30	2.21	2.13	2.05
0.328	0.314	0.302	0.293	0.284	0.276	0.270	0.265	0.260	0.255	0.251	0.247	0.246	0.243	0.240	0.237
200.0															
3.50	3.30	3.11	2.95	2.80	2.66	2.54	2.43	2.32	2.23	2.14	2.06	1.98	1.91	1.84	1.78
0.332	0.318	0.309	0.299	0.290	0.282	0.278	0.272	0.266	0.262	0.258	0.256	0.252	0.249	0.246	0.244
220.0															
2.92	2.77	2.63	2.50	2.38	2.28	2.18	2.09	2.01	1.93	1.86	1.79	1.73	1.67	1.62	1.56
0.338	0.325	0.314	0.304	0.298	0.291	0.284	0.278	0.273	0.268	0.266	0.263	0.259	0.256	0.253	0.250
240.0															
2.48	2.36	2.25	2.15	2.06	1.97	1.89	1.82	1.75	1.69	1.63	1.58	1.53	1.48	1.43	1.39
0.342	0.330	0.319	0.313	0.304	0.297	0.290	0.284	0.279	0.277	0.273	0.269	0.266	0.263	0.260	0.257
260.0															
2.14	2.04	1.95	1.87	1.80	1.73	1.66	1.60	1.55	1.50	1.45	1.40	1.36	1.32	1.28	1.24
0.346	0.338	0.327	0.318	0.310	0.303	0.296	0.293	0.289	0.284	0.280	0.276	0.273	0.269	0.266	0.266
280.0															
1.86	1.78	1.71	1.65	1.59	1.53	1.48	1.43	1.38	1.33	1.29	1.25	1.22	1.18	1.15	1.12
0.354	0.343	0.333	0.324	0.316	0.309	0.304	0.300	0.295	0.291	0.287	0.283	0.279	0.276	0.276	0.273
300.0															
1.64	1.58	1.52	1.46	1.41	1.36	1.32	1.28	1.24	1.20	1.16	1.13	1.10	1.07	1.04	1.01
0.359	0.348	0.338	0.330	0.322	0.318	0.312	0.307	0.302	0.298	0.294	0.290	0.286	0.286	0.283	0.280
320.0															
1.46	1.40	1.35	1.31	1.26	1.22	1.19	1.15	1.12	1.08	1.05	1.02	1.00	0.97	0.95	0.92
0.364	0.354	0.344	0.340	0.332	0.325	0.319	0.313	0.309	0.305	0.301	0.300	0.297	0.293	0.290	0.289

Table B2. ΔP_0 and α for chemical explosive events[a] in saturated clay shale overlain by seawater ($P_{ambient}$ = 1013 mbar).

Entries in pairs: ΔP_0—in psi, listed above; α—dimensionless, listed below.

SUMMARY OF DELTA P(0) AND ALPHA VALUES

WATER DEPTHS,FT ATTACK LISTED HORIZONTALLY ACROSS TOP

SHOCK DEPTH IN FT ATTACK LISTED VERTICALLY

	20.0	40.0	60.0	80.0	100.0	120.0	140.0	160.0	180.0	200.0	220.0	240.0	260.0	280.0	300.0	320.0
60.0	70.60	53.90	40.16	32.15	26.35	22.19	19.08	16.68	14.73	13.25	11.98	10.92	10.02	9.26	8.59	8.01
	0.352	0.304	0.302	0.294	0.290	0.288	0.282	0.281	0.278	0.276	0.274	0.274	0.272	0.271	0.270	0.268
80.0	35.94	27.47	22.58	18.84	16.05	14.00	12.35	11.04	9.96	9.06	8.30	7.66	7.10	6.61	6.18	5.81
	0.324	0.317	0.314	0.307	0.304	0.299	0.295	0.293	0.290	0.288	0.286	0.284	0.284	0.282	0.281	0.279
100.0	20.75	17.40	14.57	12.58	11.04	9.81	8.82	8.00	7.31	6.73	6.22	5.79	5.41	5.07	4.77	4.50
	0.348	0.334	0.327	0.321	0.317	0.312	0.308	0.305	0.304	0.301	0.298	0.296	0.294	0.294	0.293	0.291
120.0	13.84	11.62	10.30	9.10	8.14	7.35	6.69	6.14	5.66	5.26	4.90	4.58	4.31	4.06	3.84	3.64
	0.359	0.351	0.347	0.340	0.333	0.328	0.323	0.319	0.319	0.316	0.313	0.311	0.308	0.306	0.307	0.305
140.0	9.72	8.14	7.08	6.31	5.73	5.25	5.19	4.81	4.47	4.18	3.92	3.68	3.48	3.29	3.12	2.97
	0.361	0.359	0.356	0.352	0.350	0.350	0.346	0.342	0.341	0.338	0.335	0.332	0.330	0.328	0.328	0.326
160.0	7.86	6.57	5.72	5.07	5.27	4.68	4.51	4.20	3.93	3.69	3.47	3.28	3.11	2.95	2.81	2.68
	0.367	0.367	0.364	0.362	0.359	0.358	0.350	0.348	0.342	0.342	0.339	0.336	0.334	0.332	0.330	0.328
180.0	6.54	5.42	4.70	4.16	4.28	4.05	3.87	3.71	3.49	3.29	3.11	2.95	2.81	2.67	2.55	2.44
	0.369	0.371	0.371	0.365	0.364	0.357	0.358	0.349	0.346	0.343	0.342	0.340	0.337	0.335	0.333	0.331
200.0	5.56	5.09	4.64	4.26	4.03	3.76	3.53	3.32	3.14	2.97	2.82	2.69	2.55	2.44	2.33	2.24
	0.370	0.370	0.373	0.367	0.362	0.360	0.356	0.352	0.349	0.346	0.343	0.343	0.341	0.338	0.336	0.334
220.0	4.81	4.44	4.11	3.83	3.61	3.36	3.17	2.99	2.84	2.69	2.56	2.45	2.34	2.24	2.15	2.06
	0.370	0.372	0.375	0.369	0.364	0.360	0.359	0.355	0.352	0.349	0.346	0.343	0.343	0.341	0.339	0.337
240.0	4.25	3.91	3.64	3.42	3.23	3.08	2.87	2.72	2.59	2.46	2.35	2.25	2.15	2.07	1.98	1.91
	0.368	0.368	0.367	0.371	0.366	0.362	0.361	0.357	0.354	0.351	0.348	0.346	0.343	0.341	0.342	0.340
260.0	3.74	3.50	3.28	3.08	2.91	2.76	2.61	2.49	2.37	2.26	2.17	2.08	1.99	1.92	1.84	1.78
	0.367	0.366	0.367	0.373	0.369	0.366	0.360	0.360	0.356	0.353	0.351	0.348	0.346	0.344	0.342	0.342
280.0	3.35	3.13	2.94	2.76	2.60	2.47	2.40	2.29	2.19	2.09	2.01	1.93	1.85	1.78	1.72	1.66
	0.365	0.365	0.367	0.374	0.370	0.368	0.362	0.362	0.358	0.356	0.353	0.350	0.348	0.346	0.344	0.342
300.0	3.03	2.83	2.67	2.52	2.43	2.32	2.21	2.11	2.02	1.94	1.87	1.79	1.73	1.67	1.61	1.56
	0.368	0.367	0.369	0.375	0.371	0.370	0.364	0.360	0.360	0.357	0.355	0.352	0.350	0.348	0.346	0.344
320.0	2.75	2.57	2.42	2.29	2.20	2.10	2.02	1.94	1.89	1.81	1.74	1.68	1.62	1.56	1.51	1.46
	0.368	0.368	0.368	0.377	0.372	0.369	0.365	0.362	0.359	0.359	0.357	0.354	0.352	0.350	0.348	0.346

[a]Explosive parameters for nitromethane were used in these calculations.

Table B3. ΔP_0 and α for chemical explosive events[a] in saturated very weak coral overlain by seawater ($P_{ambient}$ = 1013 mbar).
Entries in pairs: ΔP_0 — in psi, listed above; α — dimensionless, listed below.

SUMMARY OF DELTA P(0) AND ALPHA VALUES

WATER DEPTHS, FT/4.71/3, LISTED HORIZONTALLY ACROSS TOP
ROCK DEPTHS, FT/4.71/3, LISTED VERTICALLY

	20.0	40.0	60.0	80.0	100.0	120.0	140.0	160.0	180.0	200.0	220.0	240.0	260.0	280.0	300.0	320.0
40.0	43.60	31.43	24.20	19.48	16.21	13.82	12.01	10.59	9.46	8.53	7.76	7.11	6.56	6.06	5.66	5.29
	0.336	0.324	0.316	0.309	0.303	0.300	0.296	0.293	0.292	0.290	0.286	0.286	0.285	0.283	0.283	0.282
80.0	25.07	18.17	14.58	12.55	10.81	9.47	8.41	7.55	6.85	6.25	5.75	5.32	4.96	4.62	4.33	4.07
	0.340	0.330	0.321	0.316	0.310	0.306	0.302	0.299	0.297	0.295	0.293	0.292	0.290	0.289	0.287	0.286
100.0	14.53	12.06	10.27	8.92	7.87	7.05	6.34	5.77	5.29	4.87	4.52	4.21	3.94	3.70	3.49	3.29
	0.344	0.333	0.326	0.319	0.315	0.311	0.307	0.304	0.305	0.300	0.298	0.296	0.294	0.292	0.292	0.291
120.0	10.14	8.71	7.61	6.75	6.06	5.48	5.01	4.60	4.25	3.95	3.69	3.46	3.25	3.07	2.90	2.75
	0.346	0.339	0.330	0.324	0.318	0.316	0.312	0.309	0.306	0.305	0.302	0.300	0.298	0.297	0.295	0.295
140.0	7.56	6.65	5.92	5.33	4.84	4.43	4.08	3.78	3.52	3.29	3.09	2.91	2.75	2.60	2.47	2.35
	0.347	0.338	0.331	0.327	0.322	0.318	0.316	0.313	0.310	0.307	0.307	0.304	0.302	0.301	0.299	0.297
160.0	5.90	5.28	4.77	4.34	3.98	3.68	3.41	3.18	2.98	2.80	2.64	2.50	2.37	2.25	2.14	2.04
	0.349	0.341	0.335	0.331	0.326	0.324	0.320	0.316	0.313	0.311	0.310	0.308	0.306	0.304	0.303	0.301
180.0	4.74	4.31	3.94	3.62	3.35	3.11	2.91	2.73	2.57	2.42	2.29	2.17	2.07	1.97	1.88	1.80
	0.350	0.345	0.339	0.333	0.329	0.327	0.323	0.320	0.71	0.314	0.314	0.312	0.310	0.308	0.306	0.304
200.0	3.94	3.61	3.32	3.08	2.87	2.68	2.52	2.37	2.24	2.12	2.01	1.92	1.83	1.75	1.67	1.60
	0.351	0.347	0.341	0.336	0.332	0.330	0.326	0.323	0.320	0.318	0.317	0.315	0.313	0.311	0.309	0.308
220.0	3.32	3.07	2.85	2.66	2.49	2.34	2.20	2.08	1.97	1.88	1.79	1.70	1.63	1.56	1.50	1.44
	0.353	0.349	0.345	0.339	0.334	0.333	0.329	0.326	0.323	0.321	0.321	0.318	0.316	0.314	0.313	0.311
240.0	2.85	2.65	2.47	2.32	2.19	2.06	1.95	1.85	1.76	1.68	1.60	1.53	1.47	1.41	1.35	1.30
	0.357	0.351	0.348	0.341	0.339	0.336	0.332	0.329	0.326	0.324	0.324	0.322	0.320	0.318	0.316	0.314
260.0	2.48	2.32	2.17	2.05	1.93	1.83	1.74	1.65	1.58	1.51	1.44	1.38	1.33	1.28	1.23	1.19
	0.359	0.355	0.348	0.343	0.342	0.338	0.335	0.332	0.329	0.327	0.327	0.325	0.323	0.321	0.319	0.317
280.0	2.18	2.05	1.93	1.82	1.72	1.64	1.56	1.49	1.43	1.37	1.31	1.26	1.21	1.17	1.12	1.09
	0.360	0.358	0.354	0.346	0.345	0.341	0.338	0.335	0.332	0.330	0.330	0.328	0.326	0.324	0.322	0.320
300.0	1.93	1.82	1.72	1.64	1.55	1.48	1.41	1.35	1.30	1.24	1.20	1.15	1.11	1.07	1.03	1.00
	0.362	0.359	0.356	0.351	0.347	0.344	0.341	0.338	0.335	0.333	0.333	0.331	0.329	0.327	0.325	0.323
320.0	1.73	1.63	1.55	1.48	1.41	1.35	1.29	1.25	1.19	1.14	1.10	1.06	1.02	0.99	0.95	0.92
	0.364	0.361	0.358	0.353	0.350	0.346	0.343	0.341	0.338	0.336	0.336	0.334	0.332	0.330	0.328	0.326

[a]Explosive parameters for a 6% aluminized ammonium nitrate slurry were used in these calculations.

Table B4. ΔP_0 and α for chemical explosive events[a] in saturated basalt overlain by seawater ($P_{ambient}$ = 1013 mbar); estimated medium and shock wave parameters were used in these calculations.

Entries in pairs: ΔP_0—in psi, listed above; α—dimensionless, listed below.

SUMMARY OF DELTA P(0) AND ALPHA VALUES

WATER DEPTHS, FT/KT1/3, LISTED HORIZONTALLY ACROSS TOP

ROCK DEPTHS, FT/KT1/3, LISTED VERTICALLY

	20.0	40.0	60.0	80.0	100.0	120.0	140.0	160.0	180.0	200.0	220.0	240.0	260.0	280.0	300.0	320.0
60.0	61.60	49.31	41.41	35.19	30.43	26.71	23.73	21.29	19.27	17.58	16.14	14.90	13.83	12.89	12.06	11.32
	0.261	0.234	0.215	0.202	0.191	0.183	0.177	0.172	0.168	0.164	0.161	0.158	0.155	0.153	0.151	0.149
80.0	25.64	22.17	19.47	17.31	15.55	14.10	12.87	11.83	10.94	10.16	9.48	8.88	8.35	7.87	7.45	7.06
	0.270	0.246	0.228	0.215	0.205	0.196	0.189	0.183	0.179	0.175	0.171	0.168	0.165	0.162	0.160	0.158
100.0	13.45	12.52	11.24	10.35	9.51	8.79	8.16	7.62	7.14	6.71	6.33	5.98	5.67	5.39	5.14	4.90
	0.276	0.254	0.238	0.225	0.215	0.206	0.199	0.194	0.188	0.184	0.179	0.177	0.173	0.171	0.168	0.166
120.0	8.81	8.08	7.46	6.92	6.45	6.04	5.68	5.35	5.06	4.79	4.55	4.34	4.14	3.96	3.79	3.63
	0.282	0.262	0.247	0.235	0.224	0.217	0.209	0.203	0.197	0.193	0.189	0.185	0.182	0.179	0.177	0.174
140.0	6.09	5.67	5.30	4.97	4.68	4.42	4.19	3.98	3.78	3.61	3.45	3.30	3.16	3.04	2.92	2.81
	0.288	0.270	0.255	0.244	0.234	0.225	0.217	0.212	0.206	0.202	0.197	0.193	0.191	0.188	0.185	0.182
160.0	4.47	4.20	3.96	3.75	3.56	3.38	3.22	3.08	2.95	2.82	2.71	2.60	2.51	2.41	2.33	2.25
	0.293	0.278	0.264	0.252	0.242	0.234	0.227	0.220	0.215	0.210	0.207	0.203	0.199	0.196	0.193	0.190
180.0	3.42	3.24	3.08	2.93	2.80	2.68	2.56	2.46	2.36	2.27	2.19	2.11	2.04	1.97	1.90	1.84
	0.300	0.284	0.271	0.261	0.251	0.242	0.235	0.228	0.224	0.219	0.215	0.211	0.207	0.204	0.202	0.199
200.0	2.71	2.58	2.46	2.36	2.26	2.17	2.09	2.01	1.94	1.87	1.80	1.74	1.69	1.64	1.59	1.54
	0.306	0.293	0.280	0.269	0.259	0.250	0.245	0.239	0.233	0.228	0.224	0.220	0.217	0.214	0.211	0.208
220.0	2.20	2.10	2.02	1.94	1.86	1.80	1.73	1.67	1.62	1.56	1.51	1.47	1.42	1.38	1.34	1.31
	0.314	0.300	0.287	0.277	0.269	0.261	0.253	0.247	0.242	0.237	0.234	0.230	0.226	0.223	0.219	0.216
240.0	1.82	1.75	1.68	1.62	1.56	1.51	1.46	1.41	1.37	1.33	1.29	1.25	1.22	1.18	1.15	1.12
	0.321	0.307	0.298	0.287	0.278	0.269	0.262	0.256	0.253	0.248	0.243	0.239	0.235	0.231	0.228	0.225
260.0	1.53	1.47	1.42	1.38	1.33	1.29	1.25	1.21	1.18	1.14	1.11	1.08	1.05	1.03	1.00	0.97
	0.332	0.313	0.307	0.296	0.287	0.279	0.271	0.268	0.262	0.257	0.253	0.248	0.245	0.241	0.238	0.234
280.0	1.30	1.26	1.22	1.18	1.15	1.11	1.08	1.05	1.02	0.99	0.97	0.94	0.92	0.90	0.88	0.85
	0.340	0.328	0.316	0.306	0.299	0.291	0.284	0.278	0.277	0.267	0.263	0.258	0.254	0.251	0.250	0.246
300.0	1.12	1.09	1.06	1.03	1.00	0.97	0.94	0.92	0.89	0.87	0.85	0.83	0.81	0.79	0.77	0.76
	0.350	0.338	0.329	0.319	0.310	0.302	0.294	0.288	0.283	0.278	0.273	0.269	0.267	0.263	0.260	0.257
320.0	0.98	0.95	0.92	0.90	0.88	0.85	0.83	0.81	0.79	0.77	0.75	0.74	0.72	0.70	0.69	0.67
	0.364	0.352	0.341	0.331	0.322	0.314	0.306	0.300	0.294	0.289	0.287	0.283	0.279	0.275	0.271	0.269

[a]Explosive parameters for TNT were used in these calculations.

Table B5. Observed airblast overpressures for Tugboat Events Ia and Ib.

Tugboat Ia, 1.0 ton, $D_r + D_w$ = 17.3 ft
Scaled depths: water = 30 ft/kt$^{1/3}$; coral = 143 ft/kt$^{1/3}$; α = 0.3425; ΔP_0 = 6.87 psi

$R_w/(D_r + D_w)$	ΔP (psi)	$\Delta P/\Delta P_0$
23.2	0.098	0.0143
40	0.042	0.0061
102	0.0155	0.00226
132	0.0096	0.00140
198	0.0078	0.00114
234	0.0040	0.00058
371	0.0032	0.000466
423	0.0027	0.000393
479	0.0018	0.000262

Tugboat Ib, 1.0 ton, $D_r + D_w$ = 17.9 ft
Scaled depths: water = 31 ft/kt$^{1/3}$; coral = 148 ft/kt$^{1/3}$; α = 0.3432, ΔP_0 = 6.46 psi

$R_w/(D_r + D_w)$	ΔP (psi)	$\Delta P/\Delta P_0$
17.3	0.127	0.0197
33.8	0.041	0.0063
93.4	0.014	0.00217
130.0	0.0137	0.00212
187	0.0082	0.00127
230	0.0064	0.00099
364	0.0038	0.00059
467	0.004 (?)	0.00062 (?)

Table B6. Observed airblast overpressures for Tugboat Events Ic and Id.

Tugboat Ic, 1.0 ton, $D_r + D_w = 21.7$ ft
Scaled depths: water = 38 ft/kt$^{1/3}$; coral = 179 ft/kt$^{1/3}$; $\alpha = 0.3437$; $\Delta P_0 = 4.35$ psi

$R_w/(D_r + D_w)$	ΔP (psi)	$\Delta P/\Delta P_0$
16.4	0.083	0.0191
29.4	0.040	0.0092
78.5	0.0143	0.00329
110.0	0.0078	0.00179
155	0.0056	0.00129
190	0.0040 (?)	0.00092 (?)
298	0.0030	0.000690
340	0.0028	0.000644
384	0.0036	0.000828

Tugboat Id, 1.0 ton, $D_r + D_w = 25.8$ ft
Scaled depths: water = 45 ft/kt$^{1/3}$; coral = 213 ft/kt$^{1/3}$; $\alpha = 0.3468$; $\Delta P_0 = 3.20$ psi

$R_w/(D_r + D_w)$	ΔP (psi)	$\Delta P/\Delta P_0$
10.0	0.104	0.0325
21.0	0.038	0.0119
62.5	0.0112	0.00350
94.0	0.0067	0.00209
127.0	0.0042	0.00131
163	0.0029	0.00091
255	0.0026	0.00081

Table B7. Observed airblast overpressures for Tugboat Event Ie.

Tugboat Ie, 10.0 tons, $D_r + D_w = 42.9$ ft
Scaled depths: water = 37 ft/kt$^{1/3}$; coral = 163 ft/kt$^{1/3}$; $\alpha = 0.3425$; $\Delta P_0 = 5.22$ psi

$R_w/(D_r + D_w)$	ΔP (psi)	$\Delta P/\Delta P_0$
6.5	0.259	0.0496
65.5	0.0225	0.00431
73.9	0.0185	0.00354
103.0	0.0128	0.00245
157	0.0088	0.00169
178	0.0085	0.00163
201	0.0041	0.000786

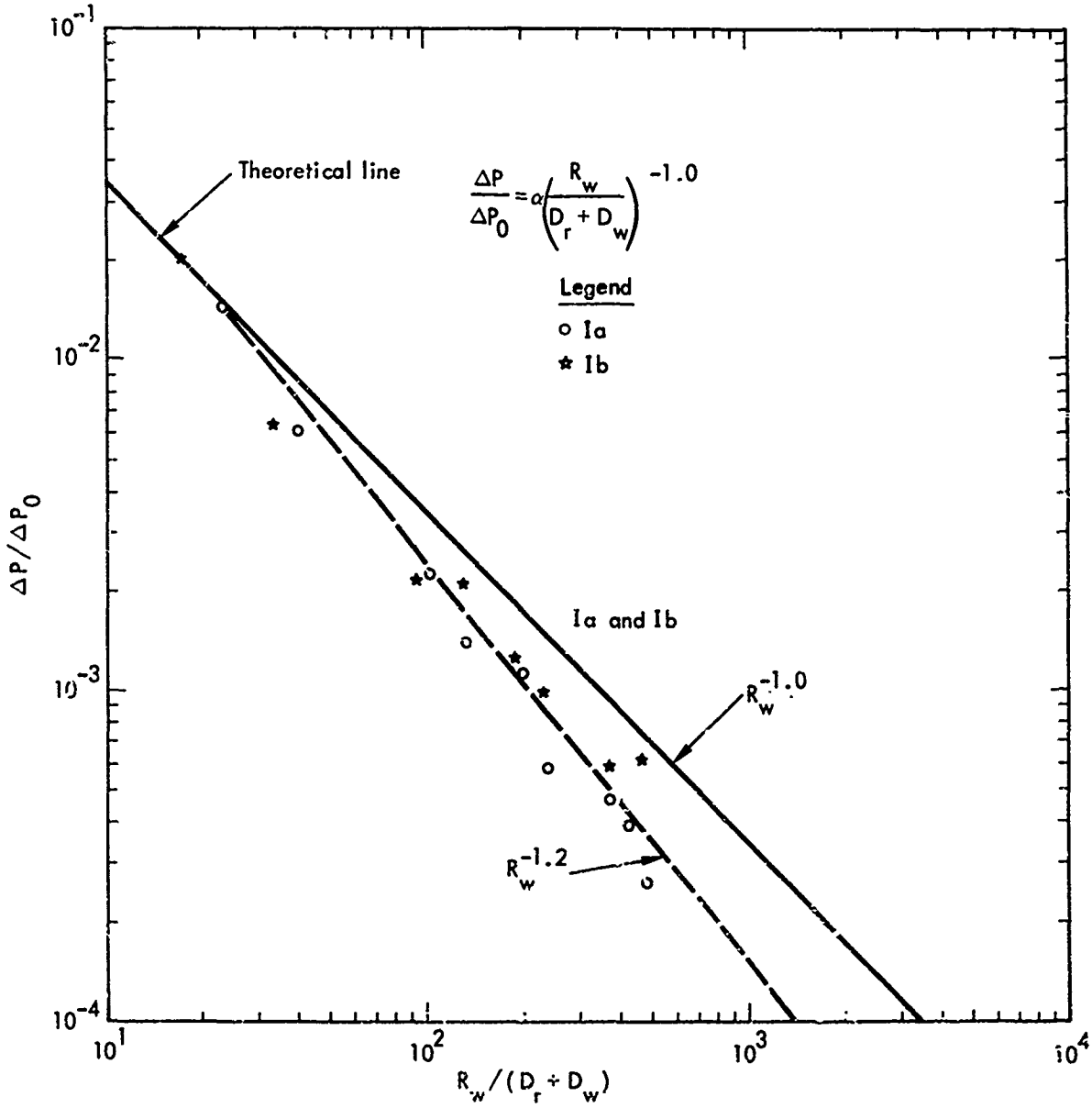

Fig. B2. Tugboat Ia and Ib (chemical explosive in coral overlain by seawater)—airblast overpressures compared to theoretical predictions.

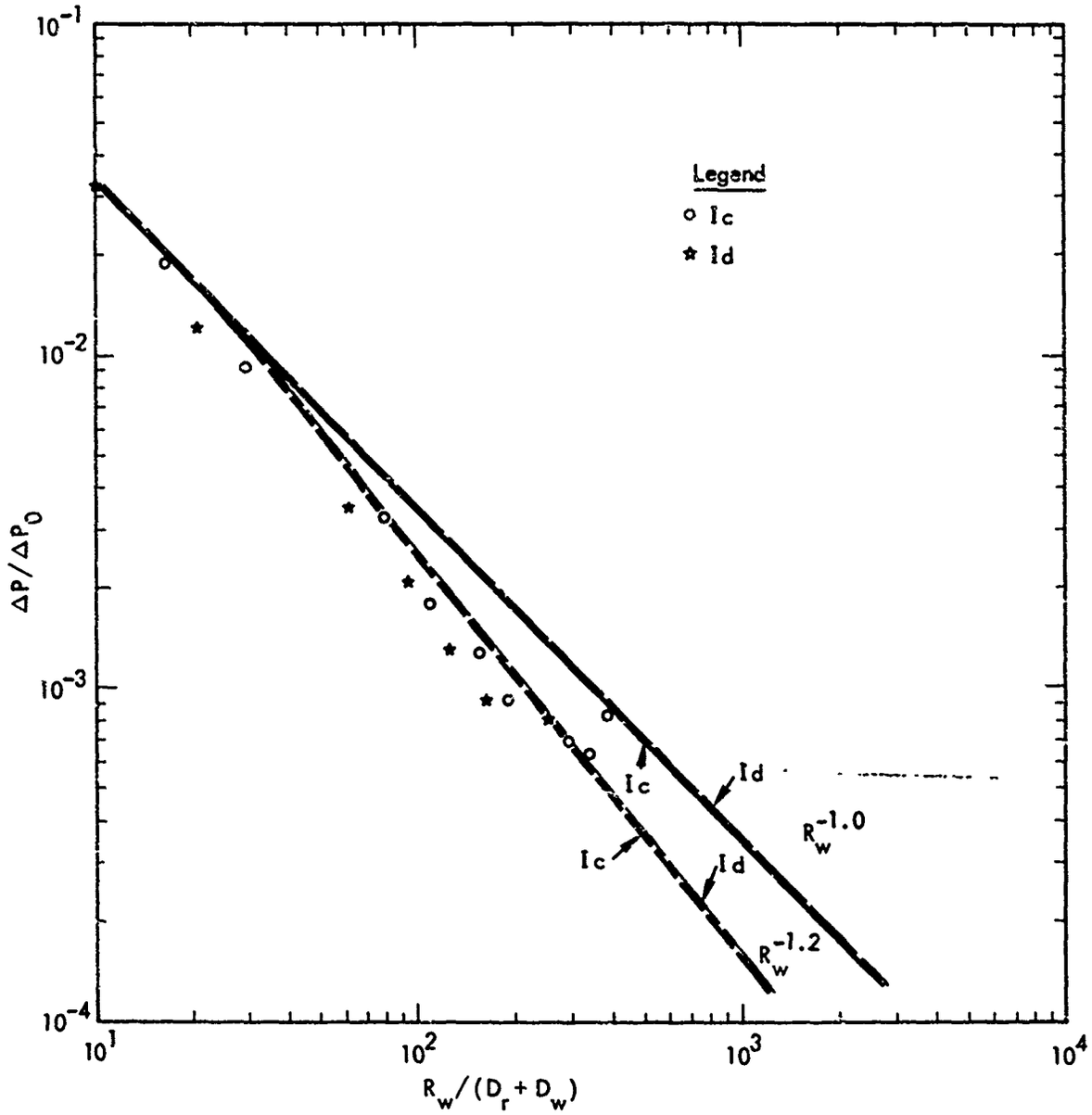

Fig. B3. Tugboat Ic and Id (chemical explosive in coral overlain by seawater) – air-blast overpressures compared to theoretical predictions.

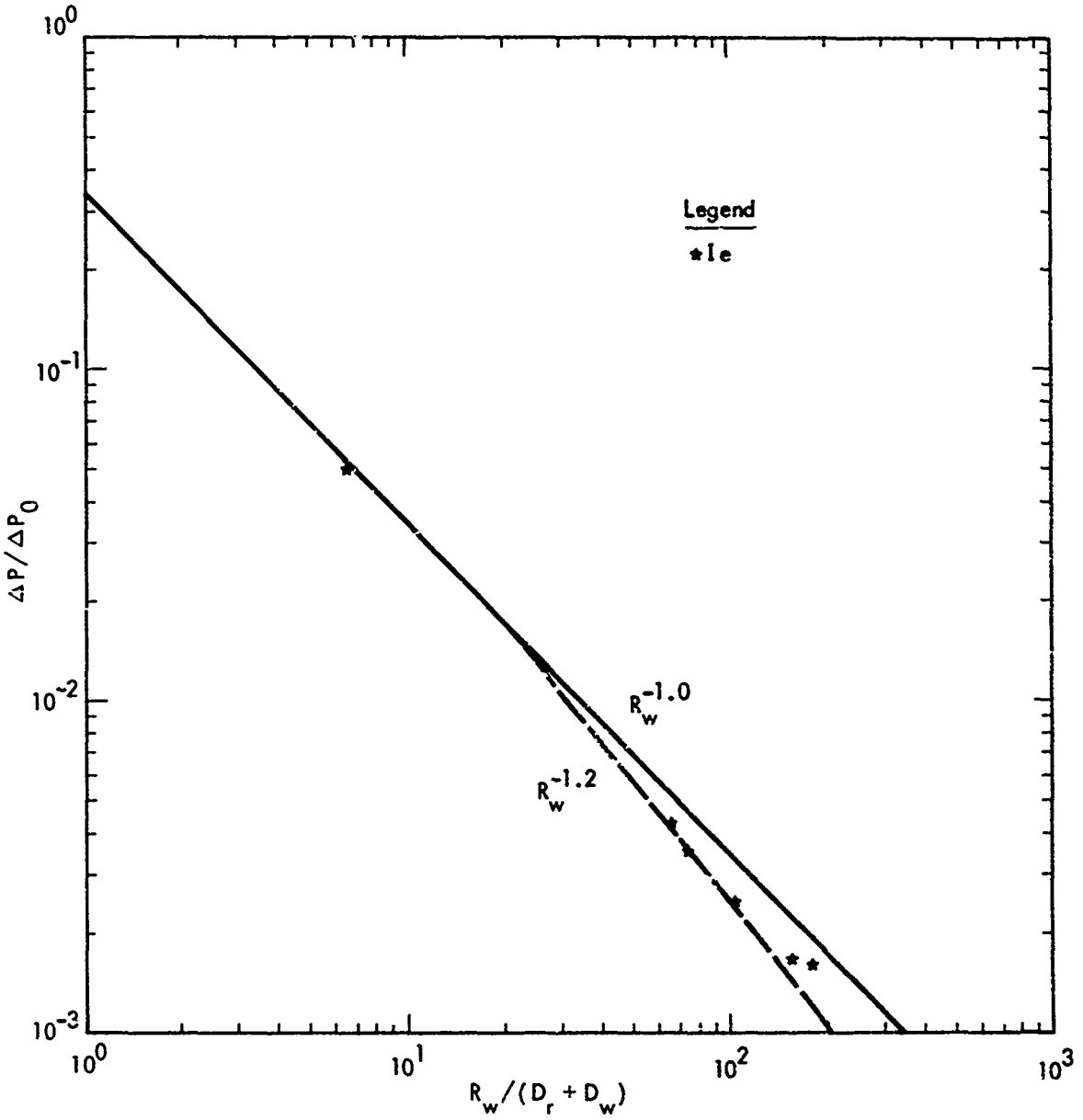

Fig. B4. Tugboat Ie (chemical explosive in coral overlain by seawater)—airblast overpressures compared to theoretical predictions.

of the peak water-shock-induced overpressures at intermediate ranges ($5 \text{ to } 10 < R_w/(D_r + D_w) < 100$), and, if possible, photographic measurements of the peak water surface spall velocities.

LIMITATIONS

MULTIMEDIA applies to single-charge detonations in a saturated cratering medium overlain by a water layer of moderate thickness. The shock transmission model, ΔP_{rock} in the cratering medium, must be known. At the present time, MULTIMEDIA must be considered a preliminary code, subject to revision and improvement of the refracted shock propagation model. Predictions thus far apply to a limited range of explosive-medium combinations, but this situation is expected to improve as more high-accuracy shock transmission data for saturated media become available from SOC-TENSOR chemical explosive modeling calculations and other sources.

```
FORTRAN                                                    1972 AD       G10/13   13.9
 4          DIMENSION XMED(14),RSUR2(90),VEL2(90),DEPW2(50),DEPR2(50),DLP02(50
 5         1,50),ALPA2(50,50)
 6          INPT=2
 7          ITPT=3
 8    C     DETERMINATION OF ALPHA, WHICH IS USED TO PERFORM MONTAN OR
 9    C     THEORETICAL AIRBLAST PREDICTIONS. THIS PROGRAM INTEGRATES
10    C     THE SURFACE VELOCITY FIELD AND CALCULATES ALPHA (AS WELL AS
11    C     OTHER IMPORTANT QUANTITIES) FOR ALL DETONATIONS IN TWO-LAYERED
12    C     MEDIA (SATURATED ROCK, ETC. OVERLAIN BY WATER)
13          RAD=1.0/57.29578
14          READ INPUT TAPE INPT,99,(XMED(N),N=1,14)
15       99 FORMAT (13A6,A2)
16          WRITE OUTPUT TAPE ITPT,100,(XMED(N),N=1,14)
17      100 FORMAT (13A6,A2/////)
18          READ INPUT TAPE INPT,101,RHOCW,CW
19          READ INPUT TAPE INPT,102,ROCR1,CR1,RTRAN,ROCR2,CR2
20          READ INPUT TAPE INPT,103,A1,B1,RTP,A2,B2
21      101 FORMAT(F5.0,F5.0)
22       02 FORMAT (5F5.0)
23      103 FORMAT (E9.0,F5.0,F5.0,E9.0,F5.0)
24          XNIN=RAD*90.00
25          READ INPUT TAPE INPT,207,PAMB
26      207 FORMAT (F8.2)
27          DO 27 II=1,16
28          DEPW=20*II
29          DEPW2(II)=DEPW
30          IKMAX=II
31          DO 27 JJ=3,16
32          DEPR=20*JJ
33          DEPR2(JJ)=DEPR
34          JKMAX=JJ
35          WRITE OUTPUT TAPE ITPT,500
36          WRITE OUTPUT TAPE ITPT,501
37          WRITE OUTPUT TAPE ITPT,502
38      500 FORMAT(10H   ANGLE  ,10H   ANGLE  ,10H  SURFACE ,10H PRESSURE ,10H
39         1 TRANSMIS ,10H PRESSURE ,10HVERTICAL  ,10HCUMULATIVE)
40      501 FORMAT(10H   ROCK   ,10H   WATER  ,10H   RANGE  ,10H  ROCK    ,10H
41         1 FACTOR   ,10H  WATER  ,10HVELOCITY  ,11HVEL PROFILE)
42      502 FORMAT(10H  DEGREES ,10H  DEGREES ,10H    FEET  ,10H   PSI    ,10H
43         1           ,10H   PSI    ,10H FT/SEC   ,10H INTEGRAL )
44          DO 216 I=1,86
45          XII=90-I
46          ANGLR=RAD*XII
47          SR=DEPR/(SINF(ANGLR))
48          IF (SR-RTRAN)217,217,218
49      217 RHOCR=ROCR1
50          CR=CR1
51          GO TO 219
52      218 RHOCR=ROCR2
53          CR=CR2
54      219 IF(SR-RTR)220,220,221
55      220 PROC=RHOCR*A1*(SR**B1)
56          GO TO 222
57      221 PROC=RHOCR*A2*(SR**B2)
58      222 CSARK=COSF(ANGLR)
59          ANGLW=ACOSF(CSARK*(CW/CR))
60          SW=DEPW/(SINF(ANGLW))
```

```
      ANGR2=XNIN-ANGLR
      ANGW2=XNIN-ANGLW
      TANGL=(2.0*RHOCW*COSF(ANGR2))/(RHOCW*COSF(ANGR2)+RHOCR*COSF(ANGW2)
     1)
      RSURF=DEPR/(TANF(ANGLR))+DEPW/(TANF(ANGLW))
      A5=DEPR/(SQRTF(RSURF))
      A6=SQRTF(TANF(ANGR2))
      A7=(DEPR)+(DEPW)*((TANF(ANGW2))*(1.0+(TANF(ANGW2))*(TANF(ANGW2))))/
     1((TANF(ANGR2))*(1.0+(TANF(ANGR2))*(TANF(ANGR2)))))
      A8=SQRTF(A7)
      A9=A5*A6/A8
      PWAT=TANGL*PROC*((A9)**1.13)
      VEL=(SINF(ANGLW))*(2.0*PWAT/(RHOCW))
      RSUR2(I)=RSURF
      VEL2(I)=VEL
      IF (I-1) 300,300,301
  300 VO=VEL2(I)
      ALPH=(VO+VEL2(I))*(RSUR2(I))
      RATIO=VO/1087.0
      GAM=1.2
      AAA=1.0
      CCC=-1.0
      BBB=GAM*RATIO
      BSQ=GAM*GAM*RATIO*RATIO
      XM=(BBB+SQRTF(BSQ-4.0*AAA*CCC))/(2.0*AAA)
  209 AM=XM
  210 DELPO=(PAMB/1013.0)*(0.01841)*AM*VO
      DLP02(II,JJ)=DELPO
      GO TO 379
  301 ALPH=ALPH+(VEL2(I)+VEL2(I-1))*(ABSF(RSUR2(I)-RSUR2(I-1)))
      DELR=RSUR2(I)-RSUR2(I-1)
      IF(DELR)711,711,379
  711 WRITE OUTPUT TAPE ITPT,714
  714 FORMAT(10X,82HINVERSION DUE TO BREAK POINT APPROX  DELTA RANGE IS
     1NEGATIVE FOR THE NEXT PRINTOUT)
  379 XANGR=ANGLR/RAD
  710 XANGW=ANGLW/RAD
      WRITE OUTPUT TAPE ITPT,400,XANGR,XANGW,RSURF,PROC,TANGL,PWAT,VEL,A
     1LPH
  400 FORMAT(8F10.3)
      VTEST=VO-50.0*VEL
      IF(VTEST)216,216,999
  216 CONTINUE
  999 ALPHA=(ALPH)*(1.0)/(2.0*3.14159*(DEPR+DEPW)*VO)
      ALPA2(II,JJ)=ALPHA
      WRITE OUTPUT TAPE ITPT,401,DEPW,DEPR,AM,VO,DELPO,ALPHA
  401 FORMAT (/12HWATER DEPTH=,F8.2,1X,8HFT/KT1/3,3X,12HROCK DEPTH= ,F8.
     12,1X,8HFT/KT1/3,3X,9HMACH NO =,F8.5,3X,17HWATER VEL AT SGZ=,F8.2,1
     1X,7HFT/SEC /18HDELTA P(O) AT SGZ=,F9.3,4H PSI,3X,6HALPHA=,F10.4///
     1/)
   27 CONTINUE
      WRITE OUTPUT TAPE ITPT,700
  700 FORMAT(1H1///////5X,38HSUMMARY OF DELTA P(O) AND ALPHA VALUES)
      WRITE OUTPUT TAPE ITPT,701
  701 FORMAT(///15X,53HWATER DEPTHS,FT/KT1/3, LISTED HORIZONTALLY ACROSS
     1 TOP)
      WRITE OUTPUT TAPE ITPT,702
  702 FORMAT(/2X,39HROCK DEPTHS, FT/KT1/3,LISTED VERTICALLY)
      WRITE OUTPUT TAPE ITPT,703,(DEPW2(IK),IK=1,IKMAX)
  703 FORMAT(//16F7.1//)
      DO 704 JK=3,JKMAX
      WRITE OUTPUT TAPE ITPT,705,DEPR2(JK)
  705 FORMAT(/1X,F5.1)
      WRITE OUTPUT TAPE ITPT,706,(DLP02(IK,JK),IK=1,IKMAX)
  706 FORMAT(16F7.2)
      WRITE OUTPUT TAPE ITPT,707,(ALPA2(IK,JK),IK=1,IKMAX)
  707 FORMAT(16F7.3)
  704 CONTINUE
   28 CALL EXIT
      END
```

Appendix C
Apparent Charge Depth

Appendix C
Apparent Charge Depth

The logical depth normalization to use in writing Eqs. (13) and (16) would be the total apparent charge depth as seen from the water layer. The total apparent charge depth, D_{ap}, for a given ray in the water layer is the depth below the water surface at which that ray, when projected back along its direction of travel in the water, intersects the vertical charge burial axis. Due to refraction at the rock-water interface, the apparent depth, D_{ap}, is not equal to the true charge burial depth ($D_r + D_w$). If C_r or $U_r > C_w$, the apparent depth will always be greater than the true depth.

The apparent depth may be determined using the law of refraction, Eq. (7). A sample solution will be performed for rays near the vertical direction, since the shock pressures and spall velocities are highest in this direction. From the law of refraction,

$$\cos \theta_r = \cos \theta_w \frac{C_r}{C_w} .$$

(In the inelastic region, U_r should be substituted for C_r in this and subsequent equations.)

For rays near the vertical direction,

$$\tan \theta_w \approx \tan \theta_r \frac{C_r}{C_w} .$$

The total apparent depth D_{ap} for a ray (near the vertical direction) that reaches the water surface at surface range R_w is then given by:

$$D_{ap} = \tan \theta_w (R_w)$$
$$\approx \tan \theta_r (C_r/C_w)(R_w) .$$

Substituting from Eq. (10) for R_w gives:

$$D_{ap} = D_r \left(\frac{C_r}{C_w}\right) + D_w \left(\frac{\tan \theta_r}{\tan \theta_w} \frac{C_r}{C_w}\right)$$

$$D_{ap} = D_r \left(\frac{C_r}{C_w}\right) + D_w = \text{constant.}$$

Let us consider only the portion of the far-field overpressure pulse produced by these rays near the vertical direction. Using the above result (D_{ap} = constant) in Eqs. 13 and 15,

$$a = \frac{1}{2\pi V_0 D_{ap}} \int_{\Delta R_w}^{\Delta R_w} V(\text{water, at } R_w)\, dR_w ,$$

where ΔR_w is a range close to SGZ (i.e., $\Delta R_w \to 0$); and

$$\Delta P = \Delta P_0 \, \alpha \, \frac{D_{ap}}{R_w} = \Delta P_0 \, \frac{1}{2\pi V_0 D_{ap}} \left(\int_{-\Delta R_w}^{\Delta R_w} V(\text{water, at } R_w) \, dR_w \right) \left(\frac{D_{ap}}{R_w} \right) .$$

The D_{ap} terms in this equation for ΔP cancel, allowing the use of any desired depth normalization in place of D_{ap}, including the true depth $D_r + D_w$ (which happens to be the most convenient). Note that the same depth normalization must be used in both the equations for α and ΔP. More generally, it can be shown that this result holds for that part of a far-field overpressure pulse ΔP produced by any small segment of the surface velocity field, whether or not the ray producing that segment is near the vertical direction. Thus, the result applies for the entire integrated surface velocity field and for α, above.

References

1. R. H. Cole, Underwater Explosions (Dover Publications, New York, 1948), pp. 14-66.
2. H. Lamb, Hydrodynamics (Dover Publications, New York, 1945), paragraphs 276-288.
3. C. M. Snell, Shockwave Interaction and Near-Surface Cavitation, Project Tugboat, USAEWES Explosive Excavation Research Laboratory, Livermore, Calif., Rept. EERO TM-71-17 (April 1972).
4. D. N. Montan, Source of Airblast from an Underground Explosion, Lawrence Livermore Laboratory, Rept. UCRL-71202 (September 1968).
5. C. M. Snell and D. L. Oltmans, Prediction of Ground-Shock-Induced Airblast Overpressures for Subsurface Explosions from Peak Vertical Spall Velocity, USAEWES Explosive Excavation Research Laboratory, Livermore, Calif., Rept. EERO TR-40 (November 1971).
6. V. E. Wheeler and R. G. Preston, Scaled Free-Field Particle Motions from Underground Explosions, Lawrence Livermore Laboratory, Rept. UCRL-50563 (August 1968).
7. H. G. Snay and A. R. Kriebel, Surface Reflection of Underwater Shock Waves, U.S. Naval Ordnance Laboratory, White Oak, Md., Rept. NOLTR 70-31 (March 1970).
8. T. R. Butkovich, J. Geophys. Res. 70, 885 (1965).
9. V. K. Shuler, Effects of Surface Reflections on Shockwave Impulse, U.S. Naval Ordnance Laboratory, White Oak, Md., Rept. NOLTR 68-138 (October 1968).
10. R. H. Gates and C. E. Gardner, Media Classification for Explosive Excavation, USAEWES Explosive Excavation Research Laboratory, Livermore, Calif., Rept. EERO TM 71-3 (September 1971).
11. H. F. Cooper and J. B. Seamon, A Geometric Technique for Studying Surface Motion from Underground Nuclear Explosions in Real Geologic Layered Media, Air Force Weapons Laboratory, Kirtland AFB, N. Mex., Rept. AFWL-TR-66-123, (January 1967).
12. J. F. Pittman, Characteristics of the Airblast Field Above Shallow Underwater Explosions, U.S. Naval Ordnance Laboratory, White Oak, Md., Rept. NAVORD 6106, (1958).
13. J. F. Goertner, Pressure Waves in the Air Above a Shallow Underwater Explosion: An Approximate Calculation By the Method of Characteristics, U.S. Naval Ordnance Laboratory, White Oak, Md., Rept. NOLTR 65-31 (December 1965).
14. C. I. Malme, J. R. Carbonell, and I. Dyer, Mechanisms in the Generation of Airblasts by Underwater Explosions, U.S. Naval Ordnance Laboratory, White Oak, Md., Rept. NOLTR 66-88 (September 1966).
15. Nuclear Weapons Blast Phenomena (U), DASA 1200, Volume 3 (Underwater Effects), Dept. of Defense, Washington, D.C., (1960) Confidential.

16. L. Rudlin and J. Silva, Airblast from Underwater Nuclear Explosions (U), U.S. Naval Ordnance Laboratory, White Oak, Md., Rept. NAVORD 6714 (February 1960), Confidential FRD.
17. D. Burton, USAEWES EERL, private communication (December 1971).
18. L. J. Vortman, Airblast from Project Tugboat Detonations, Sandia Laboratories, Albuquerque, N. Mex., Rept. SC-RR-70-541 (1970).